Aryl hydrocarbon receptor ligand production by the gut microbiota: a new therapeutic target in celiac disease

Bruno Lamas, Leticia Hernandez-Galan, Heather J Galipeau, Marco Constante, Alexandra Clarizio, Jennifer Jury, Natalia M Breyner, Alberto Caminero, Gaston Rueda, Christina L Hayes, et al.

Title: Aryl hydrocarbon receptor ligand production by the gut microbiota: a new therapeutic target in celiac disease.

Authors: Bruno Lamas[1,§], Leticia Hernandez-Galan[1,§], Heather J. Galipeau[1], Marco Constante[1], Alexandra Clarizio[1], Jennifer Jury[1], Natalia M. Breyner[1], Alberto Caminero[1], Gaston Rueda[1], Christina L. Hayes[1], Justin L. McCarville[1], Miriam Bermudez Brito[1], Julien Planchais[2], Nathalie Rolhion[3], Joseph A. Murray[4], Philippe Langella[2], Linda M.P. Loonen[5], Jerry M. Wells[5], Premysl Bercik[1], Harry Sokol[2,3,†,*] and Elena F. Verdu[1,†,*]

Affiliations:

[1]Farncombe Family Digestive Health Research Institute, Department of Medicine, McMaster University, Hamilton, Ontario, Canada.

[2]INRA, UMR1319 Micalis, AgroParisTech, Jouy-en-Josas, France.

[3]Sorbonne Université, Inserm, Centre de Recherche Saint-Antoine, CRSA, AP-HP, Hôpital Saint Antoine, Service de Gastroenterologie, F-75012 Paris, France.

[4]Division of Gastroenterology and Hepatology, Department of Immunology, Mayo Clinic College of Medicine, Rochester, Minnesota.

[5]Host-Microbe Interactomics, Animal Sciences Group, Wageningen University, Wageningen, The Netherlands.

[§]Authors share co-first authorship

[†]Authors share co-senior authorship

*****Corresponding authors:

Elena F. Verdu, MD, PhD,

Farcombe Family Digestive Health Research Institute, McMaster University, HSC 3N8, 1200 Main Street West, Hamilton, Ontario L8N 3Z5, Canada.

Email: verdue@mcmaster.ca

Tel: +1 905 525-9140

Fax: +1 905 522-3454

Harry Sokol, MD, PhD,

Gastroenterology Department, Hôpital Saint-Antoine, 184 rue du Faubourg Saint-Antoine, 75571 Paris CEDEX 12, France.

Email: harry.sokol@aphp.fr

Tel: +33 1 49 28 31 62

Fax: +33 1 49 28 31 88

Abstract: Gut microbiota metabolism of tryptophan (Trp) into derivatives that activate the aryl hydrocarbon receptor (AhR) has major role in intestinal homeostasis. Most chronic inflammatory conditions are influenced by gut microbiota cues through several pathways, and celiac disease (CeD), a loss of tolerance to dietary gluten, is no exception. We investigated whether AhR ligand production by the microbiota influences gluten immunopathology. Mice expressing the DQ8 molecule, exposed or not to gluten, were subjected to three interventions directed at enhancing the AhR pathway: 1) a diet with low or high Trp, 2) gavage with *Lactobacillus reuteri* CNCM-I5022 and CNCM-I5429 producing AhR ligands or media, and 3) treatment with either an AhR agonist or vehicle. Intestinal permeability, microbiota composition by *16S rRNA* gene sequencing, and AhR activation of intestinal contents using a reporter cell line and metabolomics, were investigated. Small intestinal pathology and inflammatory markers were measured. AhR ligands produced by the microbiota and AhR activation were determined in patients with active CeD and in controls. In mice, an enriched Trp diet shifted microbiota profiles and enhanced AhR agonist production. Experimental activation of the AhR pathway with either the enriched Trp diet, AhR ligand producers *L. reuteri*, or pharmacological stimulation using 6-formylindolo (3,2-b) carbazole (Ficz), improved gluten immunopathology. Compared with controls, CeD patients demonstrated lower intestinal AhR pathway activation, coupled with reduced capacity of the microbiota to produce AhR ligands. These results highlight a microbiota-dependent mechanism that prompt new therapeutic developments directed to the microbial modulation of the AhR pathway in celiac disease.

One sentence summary: Impaired AhR ligand production by gut microbiota decreases intestinal activation of the AhR pathway and promotes inflammation in celiac disease.

Introduction

Celiac disease (CeD) is a chronic inflammatory enteropathy that develops as a consequence of breakdown of oral tolerance to gluten in people who carry HLA-DQ2 or -DQ8 genes *(1)*. Although 40% of the worldwide population expresses one or more CeD susceptibility genes, only 1% will develop the disease *(2)*. It is currently accepted that additional environmental factors are needed to trigger the inflammatory response that will culminate in villous atrophy, and these may include microbial factors and non-gluten proteins *(3, 4)*.

The gut microbiota fosters intestinal homeostasis by modulating host immunity and physiology *(5–7)*. Disruption of microbiota composition and function, which are influenced by a variety of factors including lifestyle choices and environment, has been suggested as a key contributor to the worldwide epidemics of chronic illness, including CeD *(2, 3, 7, 8)*. Indeed, recent studies in mice have demonstrated mechanisms through which bacterial opportunistic pathogens from CeD patients and enteric viral infections directly or indirectly influence host immune responses to gluten *(4, 9, 10)*. However, only some CeD patients have a clinical history of enteric infections, suggesting other mechanisms linking microbial cues and immunological pathways may be relevant.

By-products of microbial metabolism in the gut, such as those produced through metabolism of tryptophan (Trp) from dietary sources, are emerging as key players in host-microbiota cross-talk *(11–14)*. In the gastrointestinal tract, Trp can be metabolized by the microbiota into ligands of the aryl hydrocarbon receptor (AhR) *(14–17)* as well as by host cells into kynurenine via indoleamine 2,3-dioxygenase 1 (IDO 1) *(13, 18)* or into 5-hydroxytryptamine via Trp hydroxylase 1 *(13, 19)*. AhR is a ligand-activated nuclear transcription factor widely expressed in the body and retained in an inactive complex in the

cytoplasm that after ligand binding translocates to the nucleus regulating the expression of target genes like *Cyp1a1*, *Il22* and *Il17 (14, 15)*. In this manner, AhR signaling orchestrates immune responses at barrier sites such as the gut mucosa, modulating intraepithelial lymphocytes (IEL), T cells and innate lymphoid cells (ILCs) group 3, that produce IL-17 and IL-22 *(14)*, all of which may impact CeD pathogenesis. A recent study showed that AhR expression is down-regulated in the mucosa of active CeD patients, however the relationship with the gut microbiota and mechanisms of AhR regulation, remain unknown *(20)*. Indeed, differences in composition and metabolic function of the gut microbiota between CeD patients and healthy controls have been described, including decreases in core groups known to metabolize the Trp in AhR ligands such as *Lactobacillus (21–23).* This prompted us to investigate the general hypothesis that gut microbiota in active CeD has impaired capacity to stimulate the AhR pathway.

We demonstrate that an enriched Trp diet shapes the intestinal microbiota to produce AhR ligands that reduce gluten immunopathology in genetically susceptible mice. These effects were mediated by AhR activation and observed after treatment with either *Lactobacillus reuteri* with high capacity to produce AhR ligands *(24, 25)* or, pharmacologically, using an AhR agonist. Finally, patients with active CeD exhibit lower levels of AhR agonist metabolites and decreased capacity of the microbiota to activate AhR compared with controls. The results open a previously unknown therapeutic target in CeD related to the modulation of the gut microbiota to enhance production of Trp metabolites that activate AhR.

Results

Enriched tryptophan diet shapes the microbiota to produce AhR ligands

We first investigated the capacity of enriched Trp diet to shape the microbiota after 3 weeks of dietary intervention in NOD/DQ8 mice before gluten treatment. Mice were fed a diet containing either low or enriched Trp concentration (Fig. 1A) for 3 weeks and fecal microbiota composition was analyzed. The principal coordinate analysis revealed a difference in microbiota profiles between mice fed low and enriched Trp diet (Fig. 1B) but no difference in alpha diversity was observed (fig. S1A). Mice fed the enriched Trp diet had lower relative abundance of bacteria belonging to Proteobacteria phylum such as *Bilophila*, *Desulfovibrio* and Enterobacteriaceae, and higher abundance in bacteria belonging to Firmicutes phylum such as *Lactobacillus*, *Aerococcus*, *Facklamia*, *Jeotgalicoccus* and *Staphylococcus* (Fig. 1, C and D & fig. S1B). These data suggest that high Trp diet in a gluten-naive mouse, favors the growth of bacteria considered beneficial, such as *Lactobacillus*, able to metabolize Trp into AhR ligands *(15, 17, 24)*, at the expense of potentially pro-inflammatory bacteria belonging to Proteobacteria *(26, 27)*. Trp concentration in feces was higher in mice fed the enriched Trp diet (Fig. 1E). This was associated with increased concentrations of AhR agonists including, tryptamine, indole-3-aldehyde and indole-3-lactic acid (Fig. 1E and fig. S1, C to E). A higher concentration of Trp and AhR agonists was also observed in the serum of mice fed the enriched Trp diet (fig. S1, F to I). In contrast, the concentration of kynurenine (Kyn), a Trp metabolite produced mainly by IDO 1 enzyme in host cells and implicated in chronic inflammation *(28)*, was higher in feces of mice fed the low Trp diet (Fig. 1F). Finally, the IDO activity determined by Kyn/Trp ratio, was higher in mice fed the low Trp diet (Fig. 1F). Thus, the metabolomic profile indicates that an enriched

Trp diet shapes the gut microbiota to produce AhR ligands and potentially decreases intestinal IDO 1 activity.

To investigate the functional relevance of these findings, we determined the capacity of the microbiota to activate AhR. Fecal and small intestinal contents from mice fed the enriched Trp diet induced greater activation of AhR than contents from mice fed the low Trp diet (Fig. 1G). Expression of *Cyp1a1,* an AhR target gene *(14),* was higher in the duodenum of mice fed the enriched Trp diet (Fig. 1H). Fecal lipocalin-2, duodenal *Il6* expression, IEL counts, ion transport and paracellular permeability were lower in mice fed the enriched Trp diet, suggesting an anti-inflammatory effect of the diet (Fig. 1, I to L). Thus, the production of AhR agonists by the gut microbiota of high Trp diet-fed naïve mice activates AhR, which may promote intestinal homeostasis.

Enriched tryptophan diet sustains microbial AhR activation in gluten treated mice

Gluten sensitization and challenge (D59; "gluten-treatment"; Fig 2A), regardless of dietary intervention, shifted fecal microbiota composition (fig. S2A) and alpha diversity (fig. S2, B and C) leading to increased abundance of bacteria from the Firmicutes phylum and lower abundance of bacteria belonging to the Bacteroidetes phylum (fig. S2, D to G). This was accompanied by higher AhR agonists in mice fed the enriched Trp diet (fig S3). Compared with the low Trp diet, the enriched Trp diet did not impact alpha diversity (fig. S4A), but principal coordinate analysis revealed different clustering between the two groups (Fig. 2B). Differential analysis confirmed this effect with a relative increase in bacteria belonging to the Bacteroidetes and Firmicutes phyla at the expense of bacteria from the Proteobacteria and Verrucomicrobia phyla (Fig. 2, C to D). At species level, abundance of *Bilophila*, *Desulfovibrio*, *Suturella* and

Erwinia, from the Proteobacteria phylum, was lower in the mice fed the enriched Trp diet (Fig. 2C). Among Firmicutes, *Ruminococcus gnavus* (Fig. 2C), known to produce AhR ligands *(17, 29)*, was increased in mice treated with the enriched Trp diet. In accordance, Trp and AhR agonist concentrations in feces and serum were higher in enriched Trp diet-fed mice (Fig. 2E and fig. S4, B and C). We also observed a decrease in kynurenine concentration and IDO activity in feces of enriched Trp diet-fed mice compared with low Trp diet-fed mice (Fig. 2F). Taken together these results suggest that gluten exposure was a major driver of microbiota shift, independently of Trp content in diet; however, the enriched Trp diet maintained the functional capacity to produce AhR ligands and promoted a microbiota structural profile associated with beneficial bacteria capable of AhR ligand production. The capacity of small intestine and colon content to activate AhR was higher in enriched Trp diet-fed mice compared with low Trp diet-fed mice, (Fig. 2G) and this was paralleled by higher duodenal expression of *Ahr*, and AhR target genes such as *Cyp1a1* and *Il22* (Fig. 2H). The enriched Trp diet was also associated with higher villus-to-crypt (V/C) ratios, lower IEL counts, intestinal paracellular permeability, serum fecal lipocalin-2 and duodenal *Il6* expression, but no differences in ion secretion (Fig. 2, I to L and fig. S4D). Collectively, these results support that an enriched Trp diet improves gluten immunopathology in NOD/DQ8 mice by inducing and maintaining an intestinal microbiota able to produce AhR agonists.

Lactobacillus reuteri or pharmacological-activation of AhR reduces gluten-immunopathology in mice

To investigate microbial modulation of AhR activity in the model, two previously isolated *Lactobacillus reuteri* strains that naturally exhibit high AhR-ligand production *(24, 25)*

(fig. S4E) were administered to gluten treated NOD/DQ8 mice fed either a low or enriched Trp diet (Fig. 3A). *L. reuteri* supplementation increased the capacity of the small intestinal microbiota to activate AhR in mice fed both diets, but the increase was only significant in mice fed the enriched Trp diet (Fig. 3B). *L. reuteri* supplementation decreased IEL counts in mice fed a low Trp diet compared with mice treated with media (Fig. 3C). *L. reuteri* also improved V/C ratios in mice on a low Trp diet (Fig. 3D). Taken together, these results suggest that even in the context of a low Trp diet, supplementation with *L. reuteri* may be sufficient to produce AhR ligands that modulate gluten immunopathology.

Because *L. reuteri* may have anti-inflammatory effects independent of AhR ligands, we further investigated the therapeutic potential of intestinal AhR activation, using either an AhR agonist, the 6-formylindolo (3,2-b) carbazole (Ficz) or its vehicle (Fig. 4A). After gluten treatment, mice developed higher IEL counts, lower V/C ratios, increased *Il15* expression, and barrier dysfunction (Fig. 4, B to G). Compared with basal conditions (day 0), gluten-treated mice had higher intestinal expression of *Ahr* and AhR target genes such as *Cyp1a1*, *Il22* and *Il17*, suggesting an overall state of immune activation (Fig. 4D). However, the degree of increase in *Ahr* and AhR target genes in gluten-treated NOD-DQ8 mice remained below those that were observed in control C67Bl/6 mice, particularly for *Ahr* and *Il22* (fig. S5). Moreover, higher expression of these AhR target genes was observed in NOD/DQ8 mice treated with Ficz compared with those receiving vehicle, confirming activation of AhR by the agonist (Fig. 4D). Ficz did not affect intestinal IL-15 expression (Fig. 4D), but it improved IEL counts, V/C ratios, paracellular permeability, ion transport, and other markers of overall gut inflammation (Fig. 4, B to G). Taken together, these results demonstrate that pharmacological modulation of the AhR pathway ameliorates gluten immunopathology in NOD/DQ8 mice.

Impaired AhR signaling and microbiota metabolites in patients with CeD

To study the relevance of gut microbiota-derived AhR ligands in CeD pathogenesis, we analyzed the concentrations of specific microbiota metabolites known to activate AhR in feces from patients with active CeD, patients with CeD on a gluten-free diet (GFD) for 2 years and non-celiac controls. Patients with active CeD had lower concentrations of AhR agonists including tryptamine, indole-3-aldehyde and indole-3-lactic acid (Fig. 5A and fig. S6, A to C). A higher concentration of Trp was also observed in non-celiac controls compared with patients with CeD (Fig. 5B). In contrast, xanthurenic acid and kynurenic acid, products of Trp metabolism through the kynurenine pathway, were higher in CeD patients compared with controls (Fig. 5C and fig. S6, D and E). In CeD patients treated with GFD, no difference in fecal levels of the AhR agonists tryptamine, indole-3-aldehyde and indole-3-lactic acid was observed compared with patients with active CeD (Fig. 5A and fig. S6, A to C). However, CeD patients treated with GFD had higher concentrations of indole-3-acetic acid (IAA), known to be an AhR agonist (Fig. 5D) *(13–15, 24)*. The reason for decreased fecal Trp in treated CeD patients (Fig. 5B) is unclear, but could result on the one hand, from a partially restored capacity of the gut microbiota to metabolize Trp into indoles and on the other, from a residual inflammation associated with higher Trp metabolism through the kynurenine pathway (Fig 5C and fig. S6, D and E).

To investigate the functional relevance of these findings, we studied the capacity of the microbiota to activate AhR. Consistent with the impaired production of AhR ligands, fecal samples from patients with active CeD had a lower capacity to active AhR (Fig. 5E). The capacity of the microbiota to activate AhR was rescued in CeD patients treated with the GFD

(Fig. 5E). Duodenal expression of *Ahr* and AhR pathway genes such as *Cyp1a1*, *Il22* and *Il17* was lower, while that of *Il15*, a key cytokine in CeD, was higher in active CeD patients compared with controls (Fig. 5F). Consistent with the increased production of the AhR ligand, IAA, by the microbiota of treated CeD patients, their expression of AhR pathway genes, such as *Cyp1a1* and *Il22*, was increased. Taken together, the results suggest that patients with active CeD have, on one hand impaired Trp metabolism by the gut microbiota and defective AhR activation, and on the other, higher Trp metabolism by host immune cells leading to proinflammatory kynurenine metabolites *(28, 30)* (fig. S7). In patients with CeD, the gluten-free diet partly corrects the impaired Trp metabolism by reducing the inflammation-driven kynurenine production and increasing the microbiota-dependent AhR agonist production leading to AhR activation and notably *Il22* expression, which could aid in intestinal recovery (fig. S7). These clinical data should be confirmed in a larger cohort of patients but demonstrate altered production of microbiota-derived AhR ligands in active CeD patients, suggesting a role in its pathogenesis.

Discussion

The capacity of the microbiota to produce tryptophan-based AhR ligands influences the balance between intestinal homeostasis *(13, 14, 17, 31)* and chronic inflammation, notably through impairment of IL-22-mediated anti-inflammatory mechanisms *(24, 25)*. With respect to CeD, shifts in intestinal microbial composition have been described in patients with active disease *(21–23)* but its link with AhR pathways, is unknown. Using a mouse model that develops moderate inflammation upon gluten sensitization and challenge, we show that a diet enriched in Trp, shifts the gut microbiota towards a higher abundance of *Lactobacillus* and *Ruminococcus*

gnavus, which are known AhR ligand producers *(15, 17, 24, 29)*. Metabolomic and transcriptomic analysis indicates that this shift is accompanied by an increased production of AhR ligands, as well as an activation of the AhR pathway, which promotes homeostasis and ameliorates gluten immunopathology in mice expressing CeD risk genes. Experimental modulation of the pathway with either a combination of AhR ligand producers *L. reuteri* CNCM-I5022 and CNCM-I5429 *(15, 24, 25)*, or pharmacological stimulation using Ficz, improves gluten immunopathology. Finally, relevance to human disease is demonstrated by the reduced amounts of specific microbiota metabolites, known to activate AhR, in fecal samples from patients with active CeD versus non-celiac controls. Some of these parameters are rescued by the gluten-free diet (GFD).

An AhR pathway role in CeD is indirectly supported by altered IL-17 and IL-22 production by gluten-specific T cells in a macaque model of CeD *(32)* and in biopsies of patients with CeD *(33)*. In accordance with this, we found lower expression of key genes mediating the physiological activation of AhR pathway (*Cyp1a1*, *Il22* and *Il17*) in the duodenum of patients with CeD when compared with controls. Additional support comes from *Ahr*$^{-/-}$ mice which exhibit changes in TCRαβ^{+} CD4^{+} and CD8^{+} IEL phenotypes in the colon, a subset that increases in active CeD and that responds to the gluten-free diet *(34)*. In NOD/DQ8 mice, previously described to have a genetic impairment in natural killer cells *(35)*, we observed an increase in CD3^{+} IELs during the low Trp diet, suggesting that a lower AhR activating capacity of the microbiota in the absence of dietary substrate may affect this key CeD cell subset. Finally, a recent study has shown lower AhR expression in CD4^{+}, CD8^{+} (T cells) and CD56^{+} (natural killer cells) cells isolated from both the intestinal *lamina propria* and the intraepithelial compartment of patients with active CeD *(20)*. However, the drivers for these changes, remain unknown. We

hypothesized that previously described shifts of the gut microbiota in active CeD *(21–23)* influence AhR pathways through impaired production of AhR ligands.

Lower *Lactobacillus* abundance, which include strains with known capacity to produce AhR ligands *(15, 17, 24, 25)*, has been described in the small intestine and feces of patients with active CeD *(21–23)*. On the other hand, Proteobacteria, have been reported to be overrepresented in several intestinal and extra-intestinal diseases with an inflammatory phenotype *(26, 27)*. Our previous work showed that Proteobacteria members in duodenal content of patients with CeD, such as *Pseudomonas aeruginosa*, degrade gluten differently than bacteria from healthy subjects, producing peptides that stimulate gluten-specific T cells *(9)*. In this study, enriched Trp diet shifted the microbiota of naïve NOD/DQ8 mice, towards a higher abundance of *Lactobacillus*, and decreased Proteobacteria, leading to higher production of AhR ligands that promoted intestinal homeostasis. Gluten sensitization and challenge was a major independent driver of the microbiota shift, but the capacity of the microbiota to produce AhR ligands was preserved in mice that had received the enriched Trp diet. On the other hand, the concentration of kynurenine, a Trp metabolite produced by host cells through IDO 1 and implicated in chronic inflammatory diseases *(28, 30)*, was increased in the fecal samples of mice fed the low Trp diet, as well as in the CeD patients *(36)*. Although kynurenine is an AhR agonist when used at high concentration *in vitro*, its low concentration in different animal tissues and fluids makes it unlikely to be a major AhR agonist *in vivo*, especially compared to the indoles derivatives *(13, 14, 37)*. The ability of the microbiota or host cells to metabolize Trp into AhR ligands or kynurenine respectively, depends on the availability of Trp in the gut *(13–15, 24, 25)*. Taken together, this suggests that both impaired Trp metabolism by the gut microbiota and higher Trp metabolism by host cells can lead to defective AhR signaling and increased production of kynurenine

metabolites that are associated with an inflammatory state. Based on previous studies, it is also possible that the microbiota changes induced by the enriched Trp diet impact other beneficial effects related to the microbial metabolism of immunogenic wheat proteins *(9, 10, 38)*.

To directly investigate bacterial modulation of AhR pathway in the model, we used, a combination of two *L. reuteri* strains with known AhR ligand producing capacity *(15, 24, 25)* in the context of low and enriched Trp diet. We found that *L. reuteri* supplementation increased the capacity of the small intestinal microbiota to activate AhR, particularly in mice fed the enriched Trp diet, indicating a synergism between the substrate and its metabolizer. The slight increase in AhR activity in mice fed a low Trp diet and *L. reuteri* was sufficient to improve V/C ratios and decrease IEL counts. On the other hand, *L. reuteri* supplementation in mice fed the enriched Trp diet did not improve further the beneficial effects of the enriched Trp diet, suggesting that the increased microbiota-derived endogenous production of AhR agonists induced by Trp supplementation is enough to reduce gluten immune-pathology and that further activating the pathway with *L. reuteri* does not improve the disease severity. All together, these results demonstrate that gluten immunopathology is ameliorated by dietary Trp as well as *L. reuteri* and suggest both independent, and likely shared pathways of these interventions. Our results agree with previous studies in colitis and metabolic syndrome showing that *Lactobacillus* strains capable of metabolizing Trp into AhR ligands, improve disease outcomes *(24, 25)*. Interestingly, it has recently been shown that *L. reuteri* is able to reprogram gut $CD4^+$ IEL cells into immunoregulatory T cells in an AhR-dependent manner *(39)*, suggesting a possible mechanism for improvement of intestinal barrier integrity in the context of CeD. However, we cannot rule out additional beneficial effects by *L. reuteri*, such as barrier enhancement or wheat

immunogenic peptide detoxification, as previously demonstrated for other *Lactobacillus* strains including *L. reuteri (9, 38, 40)*.

To further investigate the role of AhR activation in the improvement of gluten immunopathology, we pharmacologically modulated the AhR pathway using Ficz. Our results show that Ficz treatment improved intestinal permeability and inflammation in NOD/DQ8 treated with gluten. Studies have shown that intestinal AhR activation in mice by Ficz and/or a diet-derived AhR ligands, decrease development of colon cancer *(41)*, experimental colitis *(24, 42)* and *Citrobacter rodentium* colitis severity *(43, 44)* through IL-22 production *(14)*. Production of AhR ligands by the microbiota is required for IL-22 production *(24)*, which is involved in mucosal wound healing *(45)* and production of antimicrobial proteins by intestinal epithelial cells *(46, 47)*. Several sources of IL-22 have been identified in the gut, including Th22, TCR γδ IELs and ILCs *(46, 48)*. In this study, we observed an increased duodenal *Il22* expression after AhR signaling by Ficz or the enriched Trp diet, suggesting that the microbiota/AhR/IL-22 axis could play a role in CeD pathogenesis.

Our results are relevant to humans as impaired microbial production of AhR ligands was detected in a cohort of patients with active CeD. This was associated with reduced microbiota AhR agonist activity and reduced duodenal expression of *Ahr* and AhR pathway genes like *Il22* and *Il17*. Our results agree with a previous study showing lower AhR expression in inflamed mucosa of CeD patients *(20)* and identify a previously unreported defect in microbiota-specific AhR activation in CeD. These results raise the hypothesis that inflammation in active CeD promotes a gut microbiota shift with impaired AhR agonist production that affects IL-22 levels. Likewise, a diet low in factors that serve as substrates for microbial derived AhR ligands could contribute to CeD. This hypothesis is supported by the fact that a GFD increases the production

of AhR ligands by the microbiota, improves activation of the AhR pathway in the intestine and increases the expression of the *Il22*, known to participate in intestinal recovery *(14, 24, 25, 45, 46)*. Our study has some limitations, related to the small cohort of patients investigated as well as the fact that all the patients included in the GFD group were clinically in remission. Future studies should confirm the results in a larger cohort of patients, and also include non-responders to the GFD to investigate persistent AhR pathway abnormalities, as this would be a population of interest to target therapeutically.

In summary, our study identifies a mechanism related to the impaired production of AhR ligands by the intestinal microbiota in CeD. In mice, we show that gluten-induced pathology can be reversed through a combination of an enriched tryptophan diet and next-generation probiotics that produce AhR ligands. Therefore, in addition to providing key evidence of the importance of the microbiota composition and function in CeD pathogenesis, this study suggests that Trp catabolites derived from the metabolic activity of the intestinal microbiota could be used as biomarkers for dysbiosis and may be targeted for the development of new therapeutic approaches in CeD. These include tryptophan supplementation in combination with next generation probiotic organisms, such as *L reuteri* strains, that produce AhR ligands from the dietary substrate. Currently, the only treatment for CeD is a strict, life-long adherence to a gluten-free diet, and many suffer from persistent symptoms, despite following a GFD. The results should prompt interventional studies in humans to evaluate this therapeutic strategy in CeD patients non-responding to a GFD, but also as a preventative strategy in at-risk populations. Further interventional studies in humans are necessary to evaluate the proposed therapeutic strategy.

Materials and Methods

Study design

The objectives of the study were to investigate whether AhR ligand production by the gut microbiota influences gluten immunopathology. Several approaches were used to address this question. Transgenic SPF mice expressing the CeD DQ8 susceptibility gene were used and subjected to interventions aimed at enhancing the AhR pathways: 1) treatment with a low or high Trp diet, before and after gluten-treatment, 2) oral supplementation with AhR-ligand producing *Lactobacillus* during gluten treatment, or 3) treatment with either an AhR agonist or vehicle during gluten treatment. Gluten treatment consisted of a previously described method of sensitization and challenge, described below. Microbiota composition, AhR activation by intestinal contents, and fecal AhR ligand production were investigated in mice on low or high Trp diet, and following gluten-treatment. Signs of intestinal inflammation, AhR activation, and gluten immunopathology were examined following gluten treatment and exposure to high or low Trp diet, treatment with *Lactobacillus*, or treatment with an AhR agonist. Studies were planned with the minimum number of animals per group (n=4) to observe significant differences reproducibly. Mice were randomly assigned to groups. Statistical outliers or samples where technical issues were encountered were removed from analysis. Specific number of mice used in each experimental group are included in figure legends. In order to provide more clinical relevance, we also analyzed the concentrations of specific microbiota metabolites known to activate AhR in feces from patients with active CeD, patients with CeD on a GFD, and non-celiac controls. Subjects with inflammatory bowel, peptic ulcer, or reflux disease, as well as those taking immunosuppressants, glucocorticosteroids, antibiotics or probiotics were excluded.

Written informed consent was obtained, and the study was approved by the Hamilton Integrated Research Ethics Board. Analysis of data was performed in a blinded fashion when possible.

Gluten sensitization and challenge

Female and male 8-12 weeks old SPF NOD AB° DQ8 (NOD/DQ8) mice were bred in a conventional SPF facility at McMaster University and maintained on a gluten-free diet (Envigo, TD.05620) unless otherwise stated. All mice had unlimited access to food and water. All experiments were carried out in accordance with the McMaster University animal utilization protocols and with approval from the McMaster University Animal Care Committee and McMaster Animal Research Ethics Board (AREB). NOD/DQ8 mice were sensitized with 500 µg of pepsin-trypsin digest of gliadin (PT-gliadin) and 25 µg of cholera toxin (Sigma-Aldrich, St Louis, MO) by oral gavage once a week for 3 weeks, to break oral tolerance to gliadin *(3, 49)*. Mice were then challenged by oral gavage with 10 mg of gluten (Sigma-Aldrich) dissolved in acetic acid three times a week for 3 weeks ("gluten treatment") *(3, 49)*. Mice were sacrificed 18 to 24 hours following the final gluten challenge. In additional experiments, male and female 8-12 week-old SPF C57Bl/6 mice maintained on a normal gluten-containing chow (Envigo 2918) were included.

Probiotic and pharmacological treatments

NOD/DQ8 mice were injected i.p. with 6-formylindolo(3,2-b) carbazole (Ficz, Enzo Life Sciences, 1 µg/mouse) or vehicle (dimethyl sulfoxide, Sigma-Aldrich) at day 1, 10, 20 and 30 during gluten sensitization and challenge. For the treatments with bacteria known to produce AhR ligands *(24, 25)* mice were gavaged 6 times a week for 3 weeks with 10^9 colony-forming

units of a combination of *Lactobacillus reuteri* CNCM-I5022 and *L. reuteri* CNCM-I5429. Bacteria were grown in MRS broth supplemented with cysteine (0.5mg/mL) and Tween 80 (1mg/mL) for 18-20 h. Oral gavage with MRS was performed in control mice.

Custom tryptophan (Trp) rodent diet

NOD/DQ8 mice were fed a customized version of Envigo TD.01084 in which tryptophan concentration was adjusted at 0.1% (low Trp diet) or 1% (high Trp diet) (table S1). Three weeks after the beginning of the diets, mice were gluten sensitized and challenged.

Measurement of AhR activity

The AhR activity of human and animal stool samples was measured using a luciferase reporter assay method, as described previously *(24, 25)*. Briefly, H1L1.1c2 cells, which contained the dioxin response element-driven firefly luciferase reporter plasmid pGudLuc1.1, were seeded into a 96-well plate and stimulated with human or animal stool suspensions or small intestinal contents for 24 h. Luciferase activity was measured using a luminometer, and the results are reported as fold changes based on the negative luciferase activity of the control. All values were normalized based on the cytotoxicity of the samples using the Lactate Dehydrogenase Activity Assay (Promega, Madison, USA).

Metabolite measurements

The metabolite concentrations in stool and serum samples were determined by a specific method using HPLC-coupled to high resolution mass spectrometry as previously described *(50–52)*. IDO activity was assessed by measurement of Kyn/Trp ratio *(25, 53)*.

16S rRNA gene sequencing

Total DNA was extracted from mouse fecal samples and data were sequenced as previously described *(10)* and analyzed as previously described *(54)*. Briefly, the V3 region of the 16S ribosomal RNA gene was amplified and sequenced on the Illumina MiSeq sequencing system. Sequences obtained were aligned to each other using the Paired-End Read (PEAR) merger and *Clustering of reads into operational taxonomic units* was performed using the Quantitative Insights into Microbial Ecology (QIIME) version 1.8.0 *(55)* and data was loaded into R using the phyloseq package for downstream processing. A total of 4,012,804 reads were obtained with an average of 74,311.19 per sample and ranged from 11512 to 169,626 per sample.

Measurement of gut barrier function

Barrier function was assessed by Ussing chamber technique as previously described *(49)*. Briefly, sections of jejunum from each mouse were mounted in an Ussing Chamber with an opening of 0.6 cm^2. Net active transport across the epithelium was measured *via* a short circuit current response (I_{sc}, µA) injected through the tissue under voltage-clamp conditions. Baseline I_{sc} (µA/cm^2) was recorded at equilibrium 20 min after mounting jejunum sections. Mucosal-to-serosal transport of macromolecules was assessed by adding ^{51}Cr-EDTA in the luminal side of the chamber. ^{51}Cr-EDTA fluxes were calculated by measuring the proportion of radioactive ^{51}Cr-EDTA detected in the serosal side of the chamber after 2 hours compared to the radioactive ^{51}Cr-EDTA placed in the luminal side at the beginning of experiment.

Gene expression analysis using quantitative reverse-transcription PCR

Total RNA was isolated from human or animal duodenum samples using RNeasy Mini Kit (Qiagen, Hilden, Germany) with the DNase treatment, according to the manufacturer's instructions. RNA concentration was determined using a NanoDrop spectrophotometer (Qiagen). Quantitative RT-PCR was performed using iScript Reverse Transcriptase (Bio-Rad) and then a SsoFast EvaGreen Supermix (Bio-Rad) in a Mastercycler ep realplex apparatus (Eppendorf) with specific human or mouse oligonucleotides. Additional information on the primers used is available in table S2. qPCR data were analyzed using the $2^{-\Delta\Delta Ct}$ quantification method with human or mouse *Gapdh* as the endogenous control.

Histology and immunohistochemistry

Cross-sections of the proximal small intestine were fixed in 10% formalin and embedded in paraffin. Enteropathy was determined by measuring villus-to-crypt (V/C) ratios in a blinded fashion, as previously described *(49)*. The presence of IELs in the sections was performed by immunostaining for $CD3^+$ cells as described previously *(3, 49)*. Briefly, sections were stained with polyclonal rabbit anti-mouse CD3 (Dako) and in each section, and intraepithelial lymphocytosis was determined by counting $CD3^+$ IELs per 20 enterocytes in five randomly chosen villus tips.

Subjects and clinical cohort

Eleven patients (7 females, mean age of 36.8 years) with positive anti-tissue transglutaminase (TG2) IgA test at diagnosis attending the Adult GI Diseases Clinic at McMaster University were recruited after confirming active CeD by the presence of duodenal

atrophy (>Marsh IIIa). Patients with concurrent or past history of inflammatory bowel disease (Crohn's disease, ulcerative or undetermined colitis), as determined by laboratory, endoscopic or bowel imaging were excluded. Eighteen other patients (10 females, mean age of 51.7 years) undergoing endoscopy, in which organic disease including peptic ulcer, reflux disease, inflammatory bowel disease and celiac disease were ruled out, were recruited as *non-celiac* controls. Six patients (3 with active CeD and 3 non-celiac controls) were taking a proton pump inhibitor in the month before enrolment. An additional six CeD patients on a GFD for >2 years (4 females, mean age of 35.3) in clinical remission (with a negative anti-TG2 IgA) attending the Adult GI Disease Clinic at McMaster University were included as treated CeD patients. Patients taking immunosuppressants, glucocorticosteroids, antibiotics or probiotics were excluded. When possible, genetic analysis was performed for celiac risk genes. All the participants signed the written informed consent; fecal samples were collected and kept frozen and stored until analysis. The study was approved by the Hamilton Integrated Research Ethics Board (REB# 12-599-T). For subject demographics see table S3. Not all patients were used for all determinations due to sample availability. Specific numbers of patients included in each parameter are included in figure legends.

Statistical analysis

GraphPad Prism version 6.0 (San Diego, CA, USA) was used for all analyses and preparation of graphs. The data are presented as median (interquartile range) or mean ± SEM. Normal distribution was determined by D'Agustino-Pearson omnibus normality test, Shapiro-Wilk test and Kolmogorov-Smirnov test with Dallal-Wilkinson-Lillie correction. For data sets that failed normality tests, nonparametric tests were used to analyze significant differences.

Multiple comparisons were evaluated statistically by one-way ANOVA and *post hoc* Tukey test or nonparametric Kruskal–Wallis test followed by a *post hoc* Dunn's test. For comparisons between two groups, significance was determined using the two-tailed Student's two-tailed *t*-test or nonparametric Mann-Whitney test. In all determinations, statistical outliers (using the ROUT method), or samples where technical issues were encountered, such as poor RNA quality, poor tissue quality for Ussing chambers, or poor histological orientation were removed from analysis. Exact numbers and tests used are provided in each figure legend. Differences corresponding to $P<0.05$ were considered significant.

For microbiota analysis, R Statistics, with the stats and vegan packages, was used to perform the statistical analysis. Data transformation was used when required and possible to achieve a normal distribution (logarithmic, square root, inversion, and inverted logarithm). Differences between whole bacterial communities were tested by permutational multivariate analysis of variance (PERMANOVA) calculated using an unweighted UniFrac distance. Multiple comparisons were evaluated statistically by one-way ANOVA or Kruskall-Wallis. Statistically significant differences were then evaluated by two-tailed Student's two-tailed *t*-test or Wilcoxon rank-sum test and multiple testing was corrected via false discovery rate (FDR) estimation.

Supplementary Materials

Fig. S1. Higher fecal and serum AhR agonists in NOD/DQ8 mice fed an enriched tryptophan diet is associated with higher *Lactobacillus* abundance.

Fig. S2. Gluten treatment shifts gut microbiota of NOD/DQ8 mice regardless of diet intervention.

Fig. S3. Fecal tryptophan and AhR agonist levels before and after gluten treatment in NOD/DQ8 mice.

Fig. S4. Tryptophan supplementation increases AhR agonists in serum of gluten treated NOD/DQ8 mice.

Fig. S5. AhR and AhR pathway genes expression in C57Bl/6 and NOD/DQ8 mice.

Fig. S6. Patients with active celiac disease have lower fecal levels of AhR agonists and higher kynurenine metabolites.

Fig. S7. Proposed model for gut Trp metabolism in CeD patients.

Table S1. Low and High tryptophan (Trp) diet composition.

Table S2. qPCR primers used for gene expression analysis.

Table S3. Characteristics of the subjects and clinical cohort.

Data file S1

References and Notes

1. E. Liu, H.-S. S. Lee, C. A. Aronsson, W. A. Hagopian, S. Koletzko, M. J. Rewers, G. S. Eisenbarth, P. J. Bingley, E. Bonifacio, V. Simell, D. Agardh, Risk of pediatric celiac disease according to HLA haplotype and country. *N. Engl. J. Med.* **371**, 42–49 (2014).

2. E. F. Verdu, H. J. Galipeau, B. Jabri, Novel players in coeliac disease pathogenesis: role of the gut microbiota. *Nat. Rev. Gastroenterol. Hepatol.* **12**, 497–506 (2015).

3. H. J. Galipeau, J. L. McCarville, S. Huebener, O. Litwin, M. Meisel, B. Jabri, Y. Sanz, J. A. Murray, M. Jordana, A. Alaedini, F. G. Chirdo, E. F. Verdu, Intestinal microbiota modulates gluten-induced immunopathology in humanized mice. *Am. J. Pathol.* **185**, 2969–2982 (2015).

4. R. Bouziat, R. Hinterleitner, J. J. Brown, J. E. Stencel-Baerenwald, M. Ikizler, T. Mayassi, M. Meisel, S. M. Kim, V. Discepolo, A. J. Pruijssers, J. D. Ernest, J. A. Iskarpatyoti, L. M. M. M. Costes, I. Lawrence, B. A. Palanski, M. Varma, M. A. Zurenski, S. Khomandiak, N. McAllister, P. Aravamudhan, K. W. Boehme, F. Hu, J. N. Samsom, H.-C. C. Reinecker, S. S. Kupfer, S. Guandalini, C. E. Semrad, V. Abadie, C. Khosla, L. B. Barreiro, R. J. Xavier, A. Ng, T. S. Dermody, B. Jabri, Reovirus infection triggers inflammatory responses to dietary antigens and development of celiac disease. *Science* **356**, 44–50 (2017).

5. E. Blacher, M. Levy, E. Tatirovsky, E. Elinav, Microbiome-Modulated Metabolites at the Interface of Host Immunity. *J. Immunol.* **198**, 572–580 (2017).

6. M. Schirmer, S. P. Smeekens, H. Vlamakis, M. Jaeger, M. Oosting, E. A. Franzosa, R. T. Horst, T. Jansen, L. Jacobs, M. J. Bonder, A. Kurilshikov, J. Fu, L. A. B. A. Joosten, A. Zhernakova, C. Huttenhower, C. Wijmenga, M. G. Netea, R. J. Xavier, Linking the Human Gut Microbiome to Inflammatory Cytokine Production Capacity. *Cell* **167**, 1897 (2016).

7. N. Kamada, S.-U. U. Seo, G. Y. Chen, G. Núñez, Role of the gut microbiota in immunity and inflammatory disease. *Nat. Rev. Immunol.* **13**, 321–35 (2013).

8. A. Caminero, M. Meisel, B. Jabri, E. F. Verdu, Mechanisms by which gut microorganisms influence food sensitivities., *Nat. Rev. Gastroenterol. Hepatol.* **16**, 7–18 (2019).

9. A. Caminero, H. J. Galipeau, J. L. McCarville, C. W. Johnston, S. P. Bernier, A. K. Russell, J. Jury, A. R. Herran, J. Casqueiro, J. A. Tye-Din, M. G. Surette, N. A. Magarvey, D. Schuppan, E. F. Verdu, Duodenal Bacteria From Patients With Celiac Disease and Healthy Subjects Distinctly Affect Gluten Breakdown and Immunogenicity. *Gastroenterology* **151**, 670–683 (2016).

10. A. Caminero, J. L. McCarville, H. J. Galipeau, C. Deraison, S. P. Bernier, M. Constante, C. Rolland, M. Meisel, J. A. Murray, X. B. Yu, A. Alaedini, B. K. Coombes, P. Bercik, C. M. Southward, W. Ruf, B. Jabri, F. G. Chirdo, J. Casqueiro, M. G. Surette, N. Vergnolle, E. F. Verdu, Duodenal bacterial proteolytic activity determines sensitivity to dietary antigen through protease-activated receptor-2. *Nat. Commun.* **10**, 1198 (2019).

11. J. K. Nicholson, E. Holmes, J. Kinross, R. Burcelin, G. Gibson, W. Jia, S. Pettersson, Host-gut microbiota metabolic interactions. *Science* **336**, 1262–1267 (2012).

12. M. Levy, C. A. Thaiss, E. Elinav, Metabolites: messengers between the microbiota and the immune system. *Genes Dev.* **30**, 1589–1597 (2016).

13. A. Agus, J. Planchais, H. Sokol, Gut Microbiota Regulation of Tryptophan Metabolism in Health and Disease. *Cell Host Microbe* **23**, 716–724 (2018).

14. B. Lamas, J. M. Natividad, H. Sokol, Aryl hydrocarbon receptor and intestinal immunity. *Mucosal Immunol.* **11**, 1024–1038 (2018).

15. T. Zelante, R. G. Iannitti, C. Cunha, A. De Luca, G. Giovannini, G. Pieraccini, R. Zecchi, C. D'Angelo, C. Massi-Benedetti, F. Fallarino, A. Carvalho, P. Puccetti, L. Romani, Tryptophan

catabolites from microbiota engage aryl hydrocarbon receptor and balance mucosal reactivity via interleukin-22. *Immunity* **39**, 372–385 (2013).

16. J. E. B. E. Koper, L. M. P. M. Loonen, J. M. Wells, A. D. Troise, E. Capuano, V. Fogliano, Polyphenols and Tryptophan Metabolites Activate the Aryl Hydrocarbon Receptor in an in vitro Model of Colonic Fermentation. *Mol. Nutr. Food Res.* **63**, e1800722 (2019).

17. H. M. Roager, T. R. Licht, Microbial tryptophan catabolites in health and disease. *Nat. Commun.* **9**, 3294 (2018).

18. G. Clarke, S. Grenham, P. Scully, P. Fitzgerald, R. D. Moloney, F. Shanahan, T. G. Dinan, J. F. Cryan, The microbiome-gut-brain axis during early life regulates the hippocampal serotonergic system in a sex-dependent manner. *Mol. Psychiatry* **18**, 666–673 (2013).

19. J. M. Yano, K. Yu, G. P. Donaldson, G. G. Shastri, P. Ann, L. Ma, C. R. Nagler, R. F. Ismagilov, S. K. Mazmanian, E. Y. Hsiao, Indigenous bacteria from the gut microbiota regulate host serotonin biosynthesis. *Cell* **161**, 264–276 (2015).

20. V. Dinallo, I. Marafini, D. Di Fusco, A. Di Grazia, F. Laudisi, R. Dwairi, O. A. Paoluzi, G. Monteleone, I. Monteleone, Protective Effects of Aryl Hydrocarbon Receptor Signaling in Celiac Disease Mucosa and in Poly I:C-Induced Small Intestinal Atrophy Mouse Model. *Front. Immunol.* **10**, 91 (2019).

21. I. Nadal, E. Donat, E. Donant, C. Ribes-Koninckx, M. Calabuig, Y. Sanz, Imbalance in the composition of the duodenal microbiota of children with coeliac disease. *J. Med. Microbiol.* **56**, 1669–1674 (2007).

22. P. Wacklin, P. Laurikka, K. Lindfors, P. Collin, T. Salmi, M.-L. Lähdeaho, P. Saavalainen, M. Mäki, J. Mättö, K. Kurppa, K. Kaukinen, Altered duodenal microbiota composition in celiac

disease patients suffering from persistent symptoms on a long-term gluten-free diet. *Am. J. Gastroenterol.* **109**, 1933–1941 (2014).

23. V. D'Argenio, G. Casaburi, V. Precone, C. Pagliuca, R. Colicchio, D. Sarnataro, V. Discepolo, S. Kim, I. Russo, G. Blanco, D. Horner, M. Chiara, G. Pesole, P. Salvatore, G. Monteleone, C. Ciacci, G. Caporaso, B. Jabrì, F. Salvatore, L. Sacchetti, Metagenomics Reveals Dysbiosis and a Potentially Pathogenic N. flavescens Strain in Duodenum of Adult Celiac Patients. *Am. J. Gastroenterol.* **111**, 879–890 (2016).

24. B. Lamas, M. L. Richard, V. Leducq, H.-P. P. Pham, M.-L. L. Michel, G. Da Costa, C. Bridonneau, S. Jegou, T. W. Hoffmann, J. M. Natividad, L. Brot, S. Taleb, A. Couturier-Maillard, I. Nion-Larmurier, F. Merabtene, P. Seksik, A. Bourrier, J. Cosnes, B. Ryffel, L. Beaugerie, J.-M. M. Launay, P. Langella, R. J. Xavier, H. Sokol, CARD9 impacts colitis by altering gut microbiota metabolism of tryptophan into aryl hydrocarbon receptor ligands. *Nat. Med.* **22**, 598–605 (2016).

25. J. M. Natividad, A. Agus, J. Planchais, B. Lamas, A. C. Jarry, R. Martin, M.-L. L. Michel, C. Chong-Nguyen, R. Roussel, M. Straube, S. Jegou, C. McQuitty, M. Le Gall, G. da Costa, E. Lecornet, C. Michaudel, M. Modoux, J. Glodt, C. Bridonneau, B. Sovran, L. Dupraz, A. Bado, M. L. Richard, P. Langella, B. Hansel, J.-M. M. Launay, R. J. Xavier, H. Duboc, H. Sokol, Impaired Aryl Hydrocarbon Receptor Ligand Production by the Gut Microbiota Is a Key Factor in Metabolic Syndrome. *Cell Metab.* **28**, 737–749.e4 (2018).

26. G. Rizzatti, L. R. Lopetuso, G. Gibiino, C. Binda, A. Gasbarrini, Proteobacteria: A Common Factor in Human Diseases. *Biomed. Res. Int.* **2017**, 9351507 (2017).

27. N.-R. R. Shin, T. W. Whon, J.-W. W. Bae, Proteobacteria: microbial signature of dysbiosis in gut microbiota. *Trends Biotechnol.* **33**, 496–503 (2015).

28. G. C. Prendergast, M. Y. Chang, L. Mandik-Nayak, R. Metz, A. J. Muller, Indoleamine 2,3-dioxygenase as a modifier of pathogenic inflammation in cancer and other inflammation-associated diseases. *Curr. Med. Chem.* **18**, 2257–2262 (2011).

29. B. B. Williams, A. H. Van Benschoten, P. Cimermancic, M. S. Donia, M. Zimmermann, M. Taketani, A. Ishihara, P. C. Kashyap, J. S. Fraser, M. A. Fischbach, Discovery and characterization of gut microbiota decarboxylases that can produce the neurotransmitter tryptamine. *Cell Host Microbe* **16**, 495–503 (2014).

30. M. A. Ciorba, Indoleamine 2,3 dioxygenase in intestinal disease. *Curr. Opin. Gastroenterol.* **29**, 146–152 (2013).

31. V. Rothhammer, F. J. Quintana, The aryl hydrocarbon receptor: an environmental sensor integrating immune responses in health and disease. *Nat. Rev. Immunol.* **19,** 184-197 (2019).

32. H. Xu, S. Feely, X. Wang, D. Liu, J. Borda, J. Dufour, W. Li, P. Aye, G. Doxiadis, C. Khosla, R. Veazey, K. Sestak, Gluten-sensitive enteropathy coincides with decreased capability of intestinal T cells to secrete IL-17 and IL-22 in a macaque model for celiac disease. *Clin. Immunol.* **147**, 40–49 (2013).

33. Bodd, Ráki, Tollefsen, Fallang, Bergseng, Lundin, Sollid, HLA-DQ2-restricted gluten-reactive T cells produce IL-21 but not IL-17 or IL-22. *Mucosal Immunol.* **3**, 594–601 (2010).

34. Y. Li, S. Innocentin, D. R. Withers, N. A. Roberts, A. R. Gallagher, E. F. Grigorieva, C. Wilhelm, M. Veldhoen, Exogenous stimuli maintain intraepithelial lymphocytes via aryl hydrocarbon receptor activation. *Cell* **147**, 629–640 (2011).

35. H. Suwanai, M. A. Wilcox, D. Mathis, C. Benoist, A defective Il15 allele underlies the deficiency in natural killer cell activity in nonobese diabetic mice. *Proc. Natl. Acad. Sci. U.S.A.* **107**, 9305–9310 (2010).

36. M. I. Torres, M. A. López-Casado, P. Lorite, A. Ríos, Tryptophan metabolism and indoleamine 2,3-dioxygenase expression in coeliac disease. *Clin. Exp. Immunol.* **148**, 419–424 (2007).

37. B. Stockinger, P. Di Meglio, M. Gialitakis, J. H. H. Duarte, The aryl hydrocarbon receptor: multitasking in the immune system. *Annu. Rev. Immunol.* **32**, 403–432 (2014).

38. A. Caminero, J. L. McCarville, V. F. Zevallos, M. Pigrau, X. B. Yu, J. Jury, H. J. Galipeau, A. V. Clarizio, J. Casqueiro, J. A. Murray, S. M. Collins, A. Alaedini, P. Bercik, D. Schuppan, E. F. Verdu, Lactobacilli Degrade Wheat Amylase Trypsin Inhibitors to Reduce Intestinal Dysfunction Induced by Immunogenic Wheat Proteins. *Gastroenterology* **156**, 2266–2280 (2019).

39. L. Cervantes-Barragan, J. N. Chai, M. D. Tianero, B. Di Luccia, P. P. Ahern, J. Merriman, V. S. Cortez, M. G. Caparon, M. S. Donia, S. Gilfillan, M. Cella, J. I. Gordon, C.-S. S. Hsieh, M. Colonna, Lactobacillus reuteri induces gut intraepithelial CD4+CD8αα+ T cells. *Science* **357**, 806–810 (2017).

40. A. R. Herrán, J. Pérez-Andrés, A. Caminero, E. Nistal, S. Vivas, J. M. M. Ruiz de Morales, J. Casqueiro, Gluten-degrading bacteria are present in the human small intestine of healthy volunteers and celiac patients. *Res. Microbiol.* **168**, 673–684 (2017).

41. K. Gronke, P. P. Hernández, J. Zimmermann, C. S. N. S. Klose, M. Kofoed-Branzk, F. Guendel, M. Witkowski, C. Tizian, L. Amann, F. Schumacher, H. Glatt, A. Triantafyllopoulou, A. Diefenbach, Interleukin-22 protects intestinal stem cells against genotoxic stress. *Nature* **566,** 249-253 (2019).

42. I. Monteleone, A. Rizzo, M. Sarra, G. Sica, P. Sileri, L. Biancone, T. T. MacDonald, F. Pallone, G. Monteleone, Aryl hydrocarbon receptor-induced signals up-regulate IL-22

production and inhibit inflammation in the gastrointestinal tract. *Gastroenterology* **141**, 237–248, 248.e1 (2011).

43. C. Schiering, E. Wincent, A. Metidji, A. Iseppon, Y. Li, A. J. Potocnik, S. Omenetti, C. J. Henderson, C. R. Wolf, D. W. Nebert, B. Stockinger, Feedback control of AHR signalling regulates intestinal immunity. *Nature* **542**, 242–245 (2017).

44. J. Qiu, X. Guo, Z.-M. E. M. Chen, L. He, G. F. Sonnenberg, D. Artis, Y.-X. X. Fu, L. Zhou, Group 3 innate lymphoid cells inhibit T-cell-mediated intestinal inflammation through aryl hydrocarbon receptor signaling and regulation of microflora. *Immunity* **39**, 386–399 (2013).

45. G. Pickert, C. Neufert, M. Leppkes, Y. Zheng, N. Wittkopf, M. Warntjen, H.-A. A. Lehr, S. Hirth, B. Weigmann, S. Wirtz, W. Ouyang, M. F. Neurath, C. Becker, STAT3 links IL-22 signaling in intestinal epithelial cells to mucosal wound healing. *J. Exp. Med.* **206**, 1465–1472 (2009).

46. G. F. Sonnenberg, L. A. Fouser, D. Artis, Border patrol: regulation of immunity, inflammation and tissue homeostasis at barrier surfaces by IL-22. *Nat. Immunol.* **12**, 383–390 (2011).

47. C. Stelter, R. Käppeli, C. König, A. Krah, W.-D. D. Hardt, B. Stecher, D. Bumann, Salmonella-induced mucosal lectin RegIIIβ kills competing gut microbiota. *PLoS ONE* **6**, e20749 (2011).

48. H. Spits, D. Artis, M. Colonna, A. Diefenbach, J. Santo, G. Eberl, S. Koyasu, R. Locksley, A. McKenzie, R. Mebius, F. Powrie, E. Vivier, Innate lymphoid cells--a proposal for uniform nomenclature., *Nat. Rev. Immunol.* **13**, 145–149 (2013).

49. H. J. Galipeau, N. E. Rulli, J. Jury, X. Huang, R. Araya, J. A. Murray, C. S. David, F. G. Chirdo, K. D. McCoy, E. F. Verdu, Sensitization to gliadin induces moderate enteropathy and insulitis in nonobese diabetic-DQ8 mice. *J. Immunol.* **187**, 4338–4346 (2011).

50. A. Lefèvre, S. Mavel, L. Nadal-Desbarats, L. Galineau, S. Attucci, D. Dufour, H. Sokol, P. Emond, Validation of a global quantitative analysis methodology of tryptophan metabolites in mice using LC-MS. *Talanta* **195**, 593–598 (2019).

51. T. Hendrikx, Y. Duan, Y. Wang, J.-H. H. Oh, L. M. Alexander, W. Huang, P. Stärkel, S. B. Ho, B. Gao, O. Fiehn, P. Emond, H. Sokol, J.-P. P. van Pijkeren, B. Schnabl, Bacteria engineered to produce IL-22 in intestine induce expression of REG3G to reduce ethanol-induced liver disease in mice. *Gut* **68**, 1504–1515 (2019).

52. M. Miani, J. Le Naour, E. Waeckel-Enée, S. C. Verma, M. Straube, P. Emond, B. Ryffel, P. van Endert, H. Sokol, J. Diana, Gut Microbiota-Stimulated Innate Lymphoid Cells Support β-Defensin 14 Expression in Pancreatic Endocrine Cells, Preventing Autoimmune Diabetes. *Cell Metab.* **28**, 557–572.e6 (2018).

53. L. Laurans, N. Venteclef, Y. Haddad, M. Chajadine, F. Alzaid, S. Metghalchi, B. Sovran, R. G. P. G. Denis, J. Dairou, M. Cardellini, J.-M. M. Moreno-Navarrete, M. Straub, S. Jegou, C. McQuitty, T. Viel, B. Esposito, B. Tavitian, J. Callebert, S. H. Luquet, M. Federici, J. M. M. Fernandez-Real, R. Burcelin, J.-M. M. Launay, A. Tedgui, Z. Mallat, H. Sokol, S. Taleb, Genetic deficiency of indoleamine 2,3-dioxygenase promotes gut microbiota-mediated metabolic health. *Nat. Med.* **24**, 1113–1120 (2018).

54. M. Constante, G. Fragoso, A. Calvé, M. Samba-Mondonga, M. M. Santos, Dietary Heme Induces Gut Dysbiosis, Aggravates Colitis, and Potentiates the Development of Adenomas in Mice. *Front. Microbiol.* **8**, 1809 (2017).

55. J. G. Caporaso, J. Kuczynski, J. Stombaugh, K. Bittinger, F. D. Bushman, E. K. Costello, N. Fierer, A. G. Peña, J. K. Goodrich, J. I. Gordon, G. A. Huttley, S. T. Kelley, D. Knights, J. E. Koenig, R. E. Ley, C. A. Lozupone, D. McDonald, B. D. Muegge, M. Pirrung, J. Reeder, J. R. Sevinsky, P. J. Turnbaugh, W. A. Walters, J. Widmann, T. Yatsunenko, J. Zaneveld, R. Knight, QIIME allows analysis of high-throughput community sequencing data. *Nat. Methods* **7**, 335–336 (2010).

Acknowledgments: We thank the members of the animal facilities of McMaster University for their assistance in mouse care; and S.M. Collins, G. De Palma, M.I. Pinto-Sanchez, A. Nardelli, N. Causada Calo, J. Lu, R. Borojevic, C. Shimbori, P. Vivek, S. Rahmani, J. Dong and J.J Park for fruitful discussions and technical help. The H1L1.1c2 cell line was provided by M.S. Denison (University of California, Davis). EFV holds a Canada Research Chair in Nutrition, Inflammation and Microbiota. **Funding:** The work was supported by a Michael G. DeGroote Post-Doctoral Fellowship to B.L., a JPI HDHL Intestinal Microbiomics grant to J.W., H.S., and E.F.V. (JPI-HDHL 50-52905-98-601; ANR-15-HDIM-0001-1; CIHR-143922) and a CIHR grant to (168840) TO E.F.V. **Author contributions:** B.L., L.H.G., H.S. and E.F.V., conceived and designed the study, performed data analysis, and wrote the manuscript; B.L. and L.H.G. designed and conducted all experiments, unless otherwise indicated; M.C. analyzed the microbiota sequencing data; J.J. performed and analyzed the intestinal permeability experiments; P.E. performed the dosage of tryptophan metabolites; J.A.M., sent nonobese diabetic-DQ8 mice. A.C., J.J., H.J.G, N.M.B., A.C., C.L.H., J.L.M., J.P., N.R. and M.B.B. provided technical help for the *in vitro* and *in vivo* experiments; G.R. and P.B. provided data and samples for the patients with CeD; B.L., L.H.G., P.L., L.M.P.L., J.M.W., H.S. and E.F.V. discussed the experiments and results. **Competing interest:** B.L, J.M.W., H.S., P.L., and E.F.V. are co-inventors on a patent filed by McMaster University (PCT/CA2020/050168) on 02/08/19 titled “Methods for preventing or treating gluten-induced gastrointestinal diseases”. **Data and materials availability:** All data associated with this study are present in the paper or the Supplementary Materials.

Figure legends:

Fig. 1. Dietary tryptophan shifts gut microbiota of naïve NOD/DQ8 mice and activates the AhR pathway. A. Protocol for testing the effects of tryptophan (Trp) supplementation in NOD/DQ8 mice. **B**. Principal coordinate analysis based on bacterial *16S rRNA* gene sequence abundance in fecal content of NOD/DQ8 mice fed with low (n=10) or enriched tryptophan diet (n=9) based on UniFrac distance matrices. **C**. Heat map of the significant fecal species between low (n=10) and enriched tryptophan diets (n=10) in NOD/DQ8 mice based on the total relative abundance (Unc. = unclassified bacteria). **D**. Relative abundance, at the phylum level, in NOD/DQ8 mice fed with low (n=10) or enriched tryptophan diet (n=9). **E.** Quantification of tryptophan and total AhR agonists (tryptamine, indole-3-aldehyde and indole-3-lactic acid) in feces of NOD/DQ8 mice fed with low (n=7) or enriched tryptophan diet (n=7). **F.** Quantification of kynurenine and IDO activity (calculated by kynurenine/tryptophan ratio) in feces of NOD/DQ8 mice fed with low (n=7) or enriched tryptophan diet (n=6-7). **G**. AhR activity in feces and small intestine (SI) content of NOD/DQ8 mice fed with low (n=7-10) or enriched tryptophan diet (n=7-8). **H**. Gene expression of the AhR pathway in the proximal small intestine of NOD/DQ8 mice fed with low (n=6-7) or enriched tryptophan diet (n=5-7). **I.** Fecal lipocalin-2 quantification of NOD/DQ8 mice fed with low (n=7) or enriched tryptophan diet (n=7). **J**. Small intestinal $CD3^+$ intraepithelial lymphocytes (IEL) counts (IEL/100 enterocytes) in NOD/DQ8 mice fed with low (n=6) or enriched tryptophan diet (n=5). **K-L**. Small intestinal barrier function assessed by (**K**) ion secretion ($\mu A/cm^2$) and (**L**) paracellular permeability to ^{51}Cr-EDTA (% hot sample/h/cm^2) in NOD/DQ8 mice fed with low (n=6-8) or enriched tryptophan diet (n=6-7). Each dot represents an individual mouse and data presented as median with interquartile range and whiskers extending from minimum to maximum, or as mean + SEM. Differences in

microbial composition calculated by PERMANOVA using unweighted UniFrac distance, and significant differences between taxa evaluated by two-tailed Student's two-tailed *t*-test or Wilcoxon test and multiple testing was corrected via false discovery rate (FDR) estimation. Statistical significance in other parameters determined by Student's two-tailed *t*-test, or Mann-Whitney.

Fig. 2. Dietary tryptophan sustains AhR activation by microbiota in gluten treated mice. A. Gluten sensitization and diet protocol for testing tryptophan (Trp) supplementation in gluten treated NOD/DQ8 mice. **B**. Principal coordinate analysis based on bacterial *16S rRNA* gene sequence abundance in fecal content of gluten treated NOD/DQ8 mice fed a low (n=10) or enriched tryptophan diet (n=8) using UniFrac distance matrices. **C**. Heat map of the significant fecal species between gluten treated NOD/DQ8 mice fed low (n=10) or enriched tryptophan diet (n=8), based on the total relative abundance. **D**. Relative abundance, at the phylum level, in gluten treated NOD/DQ8 mice fed with low (n=8) or enriched tryptophan diet (n=8). **E.** Quantification of tryptophan and total AhR agonists (tryptamine, indole-3-aldehyde and indole-3-lactic acid) in feces of gluten treated NOD/DQ8 mice fed a low (n=9) or enriched tryptophan diet (n=8). **F**. Quantification of kynurenine and IDO activity, calculated by kynurenine/tryptophan ratio, in feces of gluten treated NOD/DQ8 mice fed a low (n=8-9) or enriched tryptophan diet (n=8). **G**. AhR activity in feces and small intestine (SI) content of gluten treated NOD/DQ8 mice fed a low (n=8-9) or enriched tryptophan diet (n=8). **H**. Gene expression of the AhR pathway in the proximal small intestine of gluten treated NOD/DQ8 mice fed a low (n=5-9) or enriched tryptophan diet (n=6-8). **I**. Villus-to-crypt ratios in gluten treated NOD/DQ8 mice fed a low (n=8) or enriched tryptophan diet (n=7). **J**. Small intestinal $CD3^+$ IEL

counts (IEL/100 enterocytes) in gluten treated NOD/DQ8 mice fed a low (n=6) or enriched tryptophan diet (n=6). **K**. Small intestinal paracellular permeability to ^{51}Cr-EDTA (% hot sample/h/cm^2) in gluten treated NOD/DQ8 mice fed with low (n=11) or enriched tryptophan diet (n=12). **L.** Fecal lipocalin-2 quantification in gluten treated NOD/DQ8 mice fed a low (n=14) or enriched tryptophan diet (n=14). Each dot represents an individual mouse and data presented as median with interquartile range and whiskers extending from minimum to maximum or as mean + SEM. Differences in microbial composition calculated by PERMANOVA using unweighted UniFrac distance, and significant differences between taxa evaluated by two-tailed Student's *t*-test or Wilcoxon test and multiple testing was corrected via false discovery rate (FDR) estimation. Statistical significance in other parameters determined by Student's two-tailed *t*-test, or Mann-Whitney.

Fig. 3. *Lactobacillus reuteri* rescues AhR activation and attenuates gluten immunopathology in NOD/DQ8 mice fed a low tryptophan diet. A. Protocol for dietary tryptophan (Trp) and *L. reuteri* effects. **B**. AhR activity in the small intestinal (SI) content of gluten treated NOD/DQ8 mice with and without *L. reuteri* and fed a low (n=4-5/group) or enriched tryptophan diet (n=4-5/group). **C**. Small intestinal CD3$^+$ IEL counts (IEL/100 enterocytes) in gluten treated NOD/DQ8 mice with and without *L. reuteri* and fed a low (n=5/group) or enriched tryptophan diet (n=5/group). **D**. Villus-to-crypt ratios in gluten treated NOD/DQ8 mice with and without *L. reuteri* and fed a low (n=5/group) or enriched tryptophan diet (n=5-6/group). Each dot represents an individual mouse and data presented as median with interquartile range and whiskers extending from minimum to maximum. Statistical significance determined by Student's two-tailed *t*-test, or Mann-Whitney.

Fig. 4. Treatment with a pharmacological AhR agonist reduces gluten immunopathology in NOD/DQ8 mice. A. Protocol for testing a pharmacological AhR agonist (6-formylindolo [3, 2-b] carbazole, Ficz) in gluten treated NOD-DQ8 mice. **B**. Small intestine $CD3^+$ IEL counts (IEL/100 enterocytes) in gluten treated NOD/DQ8 mice receiving a pharmacological AhR agonist (n=8) or vehicle (Day 40; n=8) and compared with non-sensitized mice at day 0 (n=8). **C**. Villus-to-crypt ratios in gluten treated NOD/DQ8 mice receiving a pharmacological AhR agonist (n=6) or vehicle (n=6) and compared with non-sensitized mice at day 0 (n=6). **D**. Gene expression of the AhR pathway in the proximal small intestine of gluten treated NOD/DQ8 mice receiving a pharmacological AhR agonist (n=7-8) or vehicle (n=7-8) and compared with non-sensitized mice at day 0 (n=6-8). **E-F**. Small intestinal barrier function assessed by (**E**) paracellular permeability to ^{51}Cr-EDTA flux (% hot sample/h/cm^2) and (**F**) ion secretion (µA/cm^2) in gluten treated NOD/DQ8 mice receiving a pharmacological AhR agonist (n=7) or vehicle (n=8) and compared with non-sensitized mice at day 0 (n=7-8). **G**. Quantification of fecal lipocalin-2 in gluten treated NOD/DQ8 mice receiving a pharmacological AhR agonist (n=5) or vehicle (n=5). Each dot represents an individual mouse and data presented as median with interquartile range and whiskers extending from minimum to maximum or as mean + SEM. Statistical significance determined by one-way ANOVA with Tukey *post hoc* test, Kruskal–Wallis followed by a Dunn's *post hoc* test, or Mann-Whitney.

Fig. 5. Celiac patients (CeD) show decreased AhR activation and lower concentration of fecal AhR agonist than controls. A-D. Quantification of (**A**) total AhR agonists (tryptamine, indole-3-aldehyde and indole-3-lactic acid), (**B**) tryptophan and (**C**) total kynurenine metabolites (xanthurenic and kynurenic acid) and (**D**) indole-3-acetic acid (IAA) in fecal samples in patients

with active (n=10) or treated (GFD; n=6) celiac disease (CeD) and non-celiac controls (n=13). **E**. AhR activity in fecal samples of patients with active (n=10) or treated (GFD; n=6) CeD and non-celiac controls (n=13). **F**. Gene expression of the AhR pathway in duodenal biopsy from patients with active (n=4-6) or treated (GFD; n=3-5) CeD and non-celiac controls (n=5). Each dot represents an individual human subject and data presented as median with interquartile range and whiskers extending from minimum to maximum, or mean + SEM. Statistical significance for AhR agonists and IAA determined by Mann-Whitney or Student's two-tailed *t*-test, respectively; other parameters determined by one-way ANOVA with Tukey *post hoc* test, or Kruskal–Wallis followed by a Dunn's *post hoc* test or Mann-Whitney.

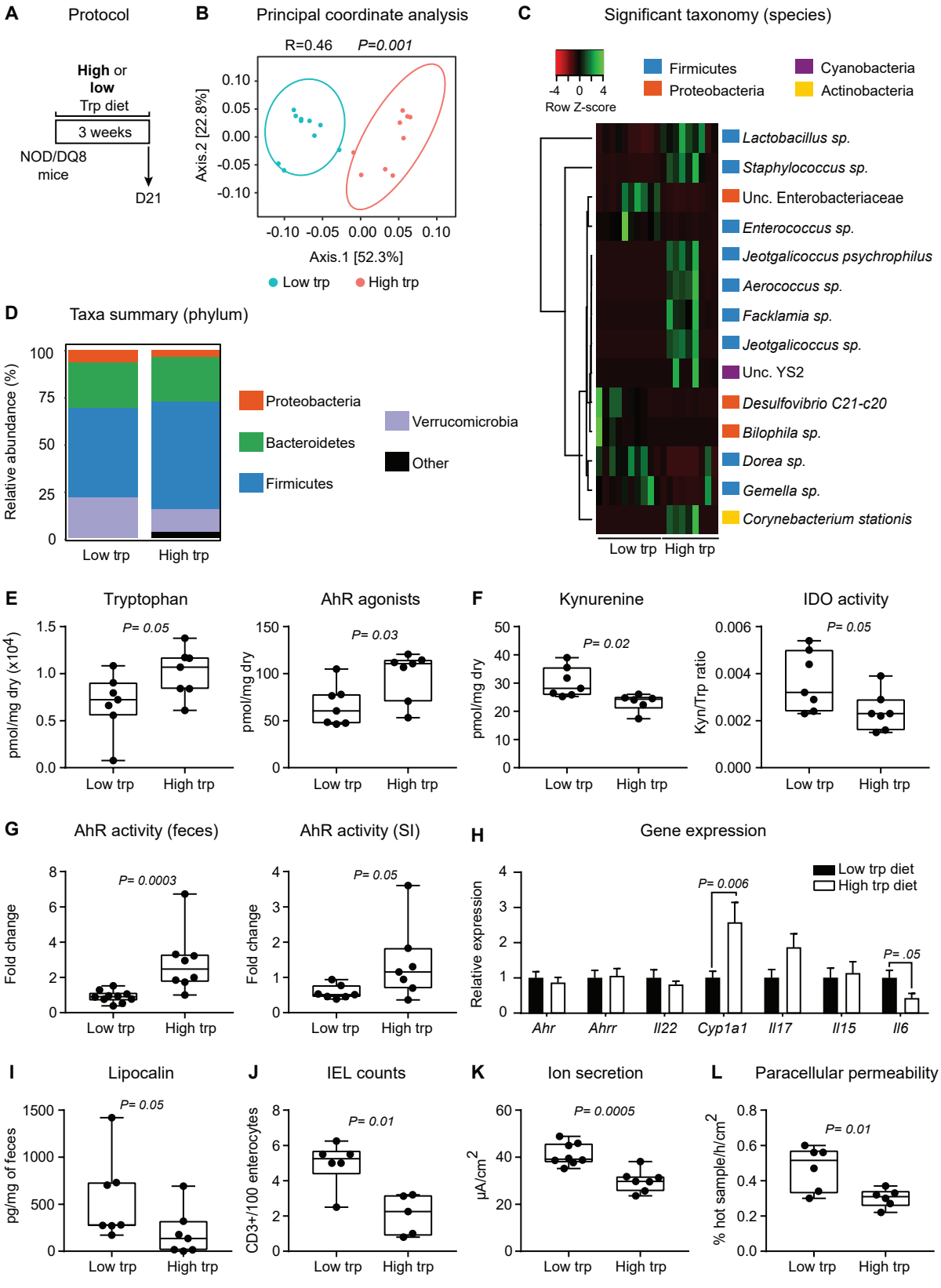
A
Protocol
High or low Trp diet
3 weeks
NOD/DQ8 mice
D21
B
Principal coordinate analysis
R=0.46
P=0.001
Axis.2 [22.8%]
Axis.1 [52.3%]
Low trp
High trp
C
Significant taxonomy (species)
Row Z-score
Firmicutes
Proteobacteria
Cyanobacteria
Actinobacteria
Lactobacillus sp.
Staphylococcus sp.
Unc. Enterobacteriaceae
Enterococcus sp.
Jeotgalicoccus psychrophilus
Aerococcus sp.
Facklamia sp.
Jeotgalicoccus sp.
Unc. YS2
Desulfovibrio C21-c20
Bilophila sp.
Dorea sp.
Gemella sp.
Corynebacterium stationis
D
Taxa summary (phylum)
Relative abundance (%)
Proteobacteria
Bacteroidetes
Firmicutes
Verrucomicrobia
Other
E
Tryptophan
pmol/mg dry (x10^4)
P= 0.05
AhR agonists
pmol/mg dry
P= 0.03
F
Kynurenine
pmol/mg dry
P= 0.02
IDO activity
Kyn/Trp ratio
P= 0.05
G
AhR activity (feces)
Fold change
P= 0.0003
AhR activity (SI)
P= 0.05
H
Gene expression
Low trp diet
High trp diet
Relative expression
P= 0.006
P= .05
Ahr
Ahrr
Il22
Cyp1a1
Il17
Il15
Il6
I
Lipocalin
pg/mg of feces
P= 0.05
J
IEL counts
CD3+/100 enterocytes
P= 0.01
K
Ion secretion
µA/cm^2
P= 0.0005
L
Paracellular permeability
% hot sample/h/cm^2
P= 0.01
Low trp
High trp

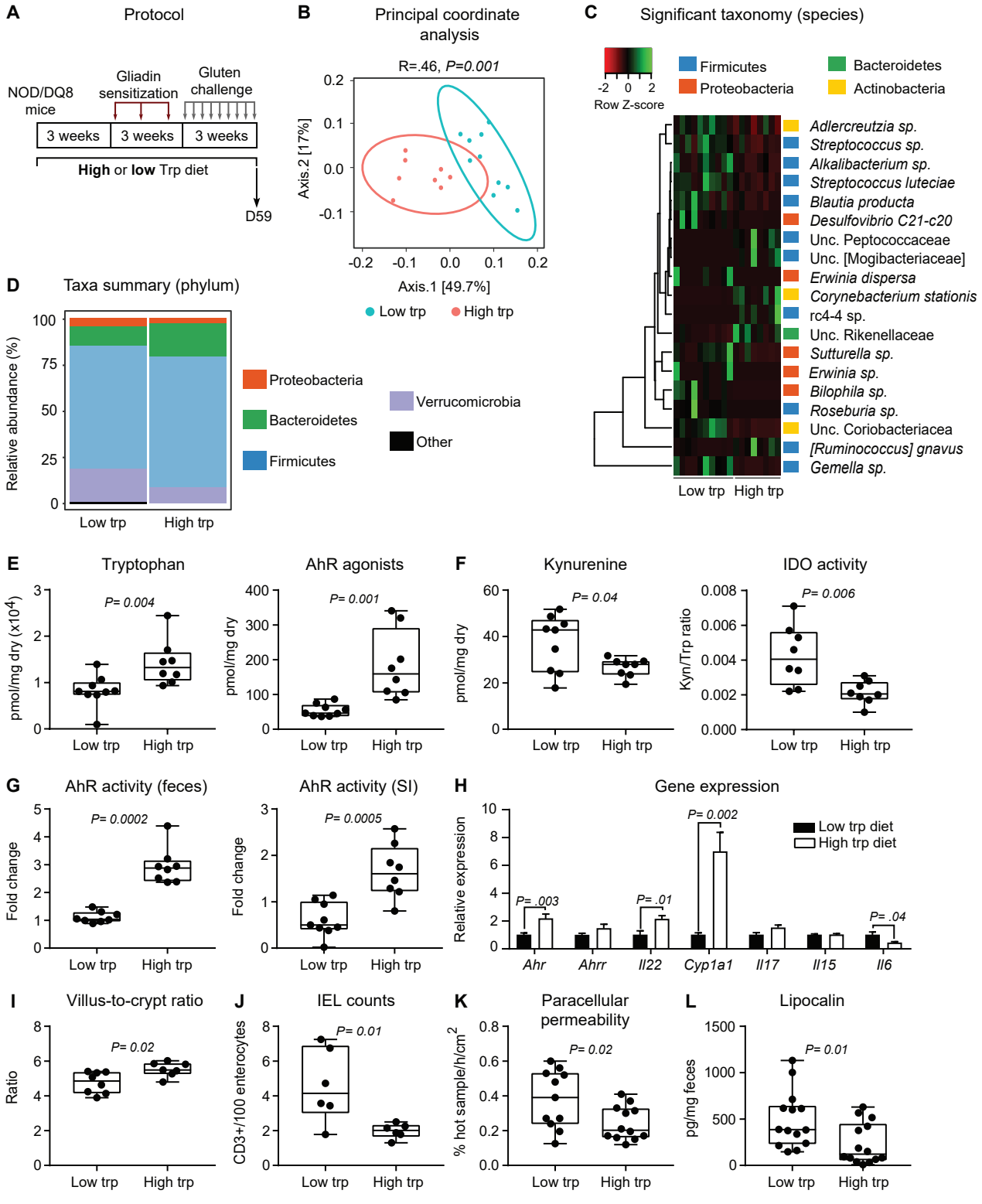
A
Protocol
NOD/DQ8 mice
Gliadin sensitization
Gluten challenge
3 weeks
3 weeks
3 weeks
High or low Trp diet
D59
B
Principal coordinate analysis
R=.46, P=0.001
Axis.2 [17%]
Axis.1 [49.7%]
Low trp
High trp
C
Significant taxonomy (species)
Row Z-score
Firmicutes
Proteobacteria
Bacteroidetes
Actinobacteria
Adlercreutzia sp.
Streptococcus sp.
Alkalibacterium sp.
Streptococcus luteciae
Blautia producta
Desulfovibrio C21-c20
Unc. Peptococcaceae
Unc. [Mogibacteriaceae]
Erwinia dispersa
Corynebacterium stationis
rc4-4 sp.
Unc. Rikenellaceae
Sutturella sp.
Erwinia sp.
Bilophila sp.
Roseburia sp.
Unc. Coriobacteriacea
[Ruminococcus] gnavus
Gemella sp.
Low trp
High trp
D
Taxa summary (phylum)
Relative abundance (%)
Proteobacteria
Bacteroidetes
Firmicutes
Verrucomicrobia
Other
Low trp
High trp
E
Tryptophan
pmol/mg dry (x10^4)
P= 0.004
AhR agonists
pmol/mg dry
P= 0.001
F
Kynurenine
pmol/mg dry
P= 0.04
IDO activity
Kyn/Trp ratio
P= 0.006
G
AhR activity (feces)
Fold change
P= 0.0002
AhR activity (SI)
Fold change
P= 0.0005
H
Gene expression
Relative expression
Low trp diet
High trp diet
P= .003
P= .01
P= 0.002
P= .04
Ahr
Ahrr
Il22
Cyp1a1
Il17
Il15
Il6
I
Villus-to-crypt ratio
Ratio
P= 0.02
J
IEL counts
CD3+/100 enterocytes
P= 0.01
K
Paracellular permeability
% hot sample/h/cm^2
P= 0.02
L
Lipocalin
pg/mg feces
P= 0.01

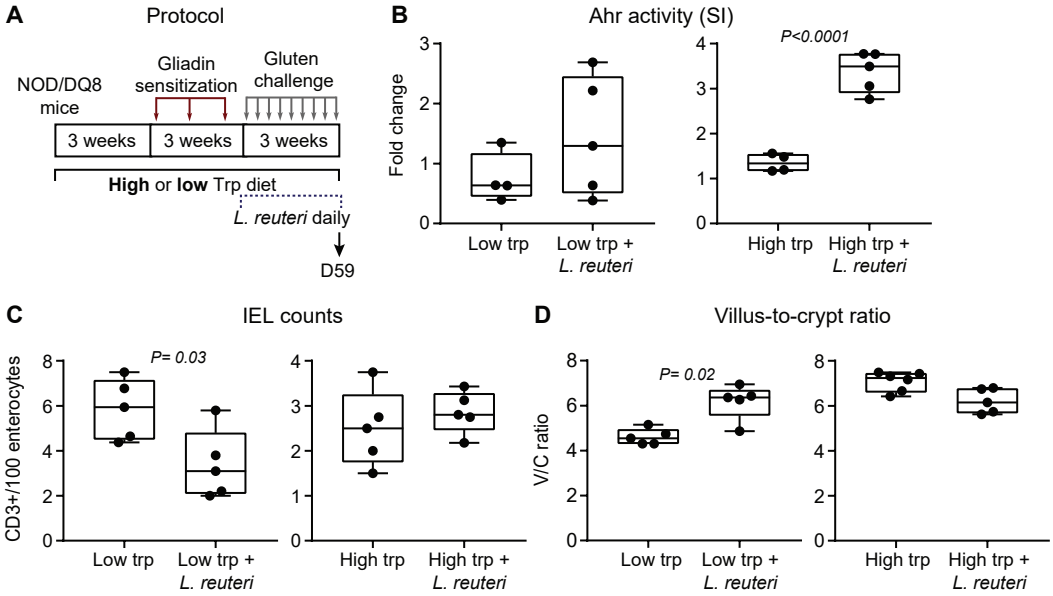
A
Protocol
NOD/DQ8 mice
Gliadin sensitization
Gluten challenge
3 weeks
3 weeks
3 weeks
High or low Trp diet
L. reuteri daily
D59
B
Ahr activity (SI)
Fold change
Low trp
Low trp + L. reuteri
P<0.0001
High trp
High trp + L. reuteri
C
IEL counts
CD3+/100 enterocytes
P= 0.03
Low trp
Low trp + L. reuteri
High trp
High trp + L. reuteri
D
Villus-to-crypt ratio
V/C ratio
P= 0.02
Low trp
Low trp + L. reuteri
High trp
High trp + L. reuteri

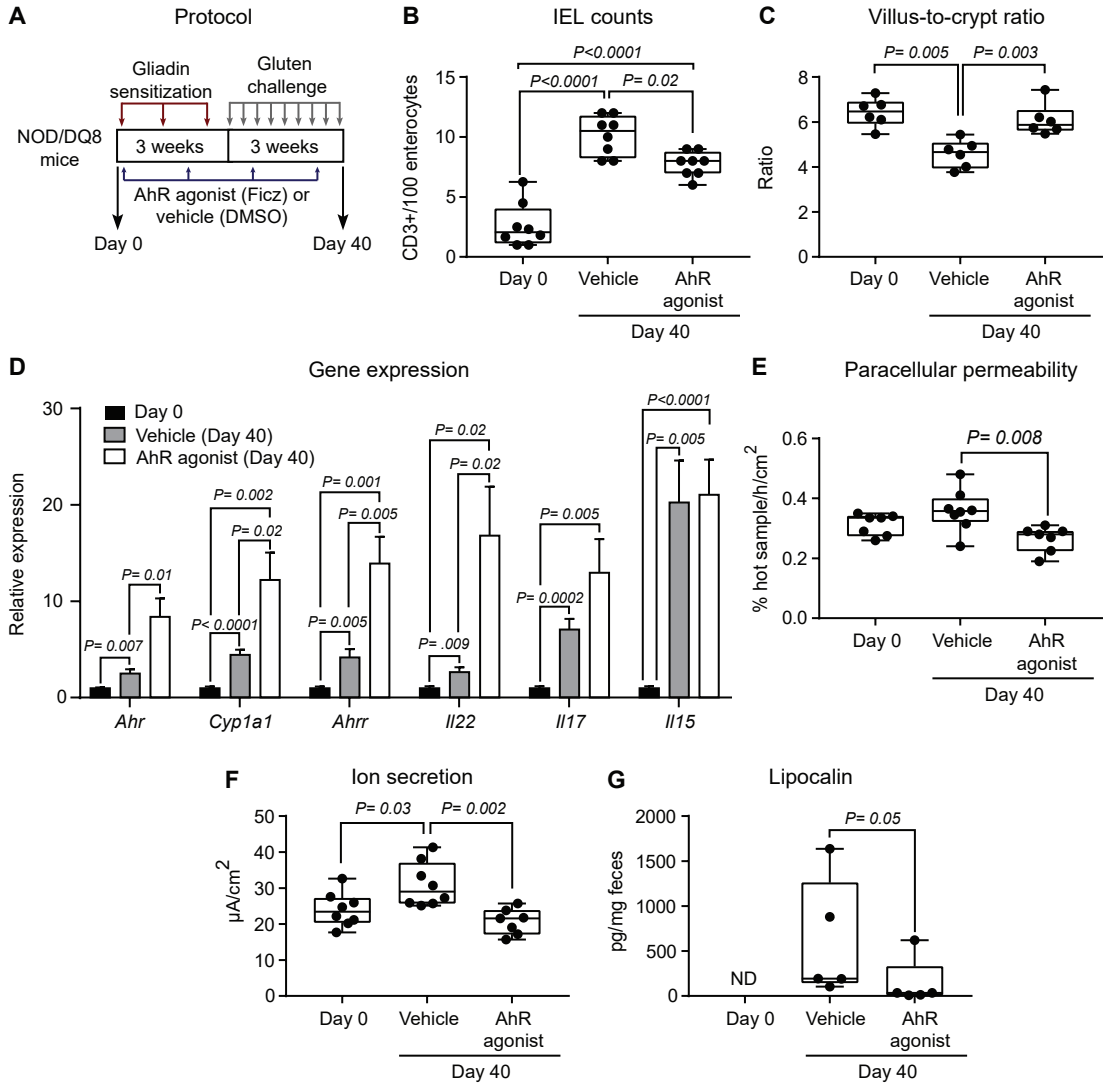
A
Protocol
Gliadin sensitization
Gluten challenge
NOD/DQ8 mice
3 weeks
3 weeks
AhR agonist (Ficz) or vehicle (DMSO)
Day 0
Day 40
B
IEL counts
CD3+/100 enterocytes
P<0.0001
P<0.0001
P= 0.02
Day 0
Vehicle
AhR agonist
Day 40
C
Villus-to-crypt ratio
Ratio
P= 0.005
P= 0.003
Day 0
Vehicle
AhR agonist
Day 40
D
Gene expression
Relative expression
Day 0
Vehicle (Day 40)
AhR agonist (Day 40)
P= 0.007
P= 0.01
P< 0.0001
P= 0.002
P= 0.02
P= 0.005
P= 0.001
P= 0.005
P= .009
P= 0.02
P= 0.02
P= 0.0002
P= 0.005
P<0.0001
P= 0.005
Ahr
Cyp1a1
Ahrr
Il22
Il17
Il15
E
Paracellular permeability
% hot sample/h/cm2
P= 0.008
Day 0
Vehicle
AhR agonist
Day 40
F
Ion secretion
µA/cm2
P= 0.03
P= 0.002
Day 0
Vehicle
AhR agonist
Day 40
G
Lipocalin
pg/mg feces
P= 0.05
ND
Day 0
Vehicle
AhR agonist
Day 40

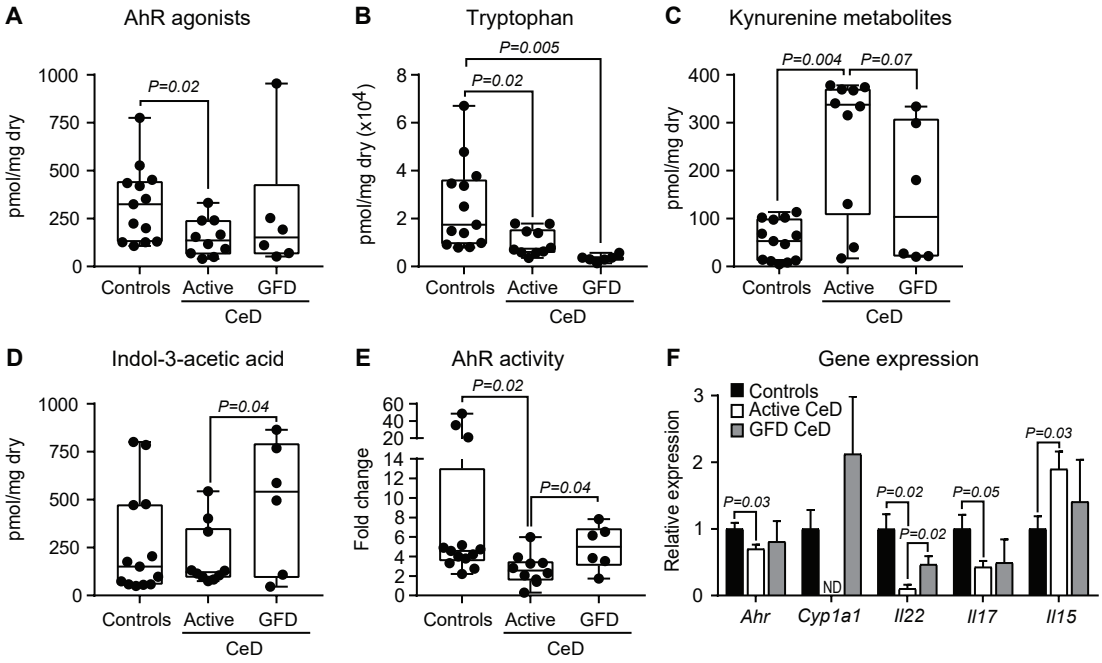
A
AhR agonists
pmol/mg dry
P=0.02
Controls
Active
GFD
CeD
B
Tryptophan
pmol/mg dry (x10^4)
P=0.005
P=0.02
C
Kynurenine metabolites
pmol/mg dry
P=0.004
P=0.07
D
Indol-3-acetic acid
P=0.04
E
AhR activity
Fold change
P=0.02
P=0.04
F
Gene expression
Relative expression
Controls
Active CeD
GFD CeD
P=0.03
P=0.02
P=0.02
P=0.05
P=0.03
ND
Ahr
Cyp1a1
Il22
Il17
Il15

Supplementary Material

Figure S1

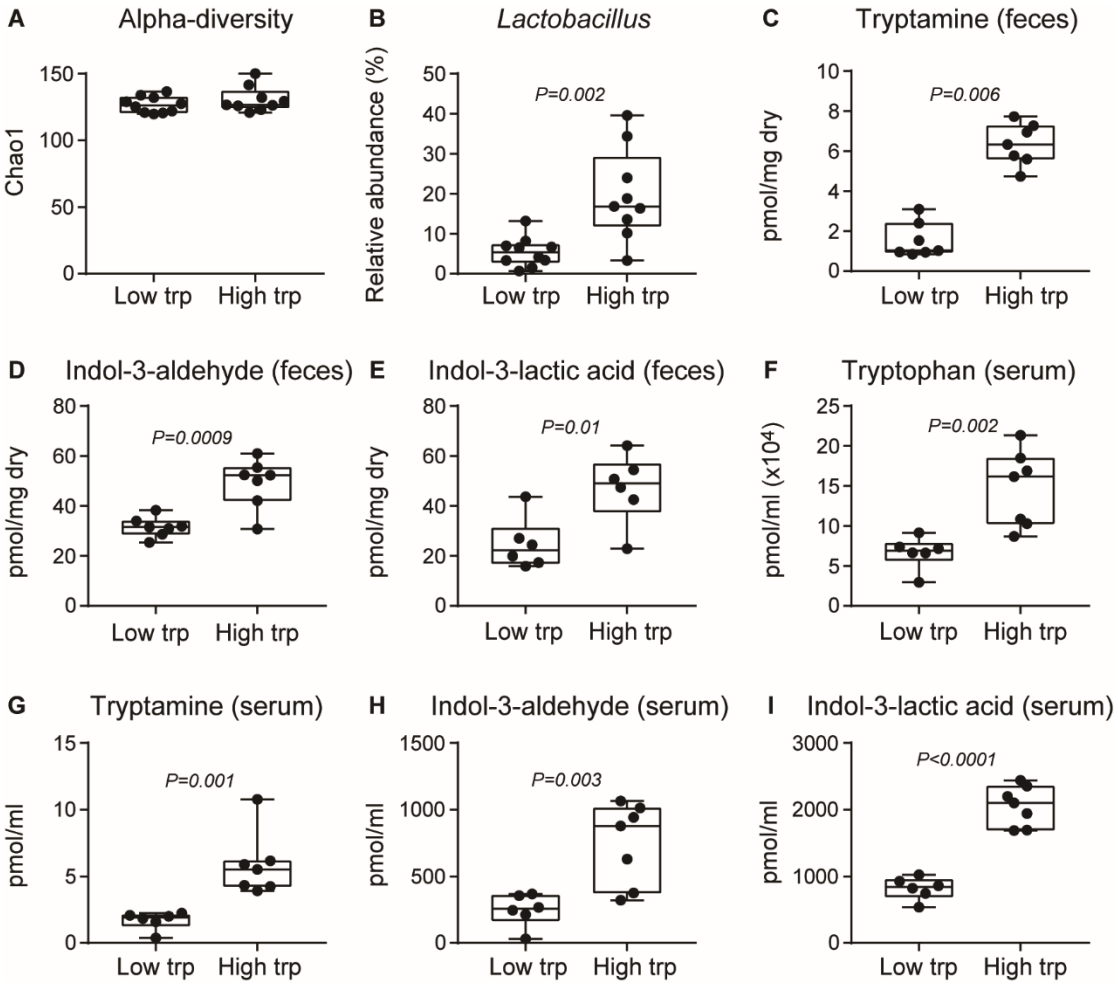

Figure S1. Higher fecal and serum AhR agonists in NOD/DQ8 mice fed an enriched tryptophan diet is associated with higher *Lactobacillus* abundance. **A**. Alpha-diversity of fecal microbiota of NOD/DQ8 mice fed a low (n=10) or enriched tryptophan (Trp) diet (n=9). **B**. Diet-specific fecal changes in *Lactobacillus* relative abundance. **C-E.** Fecal quantification of (**C**) tryptamine (**D**) indole-3-aldehyde and (**E**) indole-3-lactic acid in NOD/DQ8 mice fed a low (n=6-7) or enriched tryptophan diet (n=6-7). **F-I**. Serum quantification of (**F**) tryptophan, (**G**) tryptamine, (**H**) indole-3-aldehyde and (**I**) indole-3-lactic acid) in NOD/DQ8 mice fed a low

(n=6) or enriched tryptophan diet (n=7). Each dot represents an individual mouse and data presented as median with interquartile range and whiskers extending from minimum to maximum. Statistical significance determined by Student's two-tailed *t*-test, or Mann-Whitney.

Figure S2

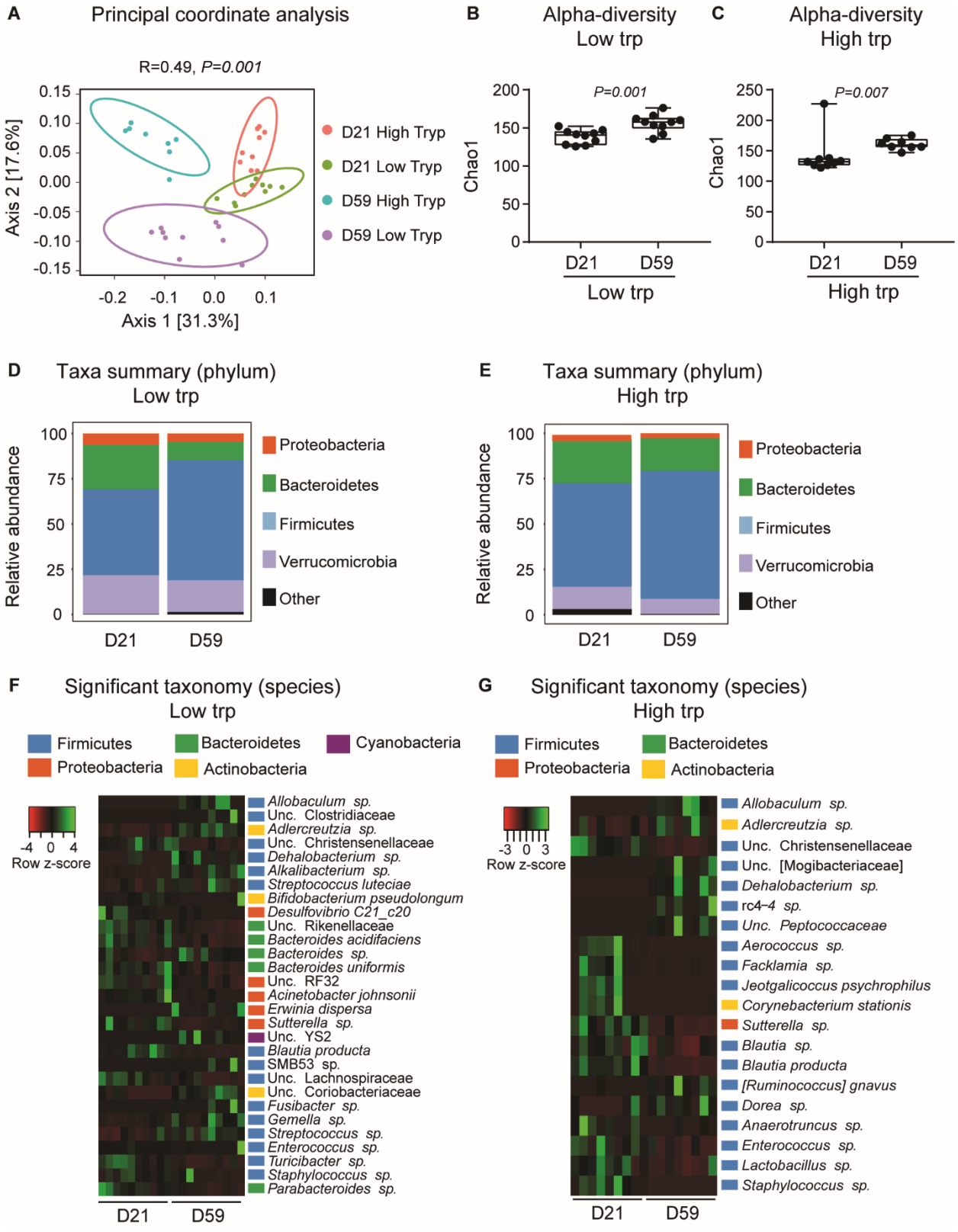
A
Principal coordinate analysis
R=0.49, P=0.001
Axis 2 [17.6%]
Axis 1 [31.3%]
D21 High Tryp
D21 Low Tryp
D59 High Tryp
D59 Low Tryp
B
Alpha-diversity
Low trp
P=0.001
Chao1
D21
D59
Low trp
C
Alpha-diversity
High trp
P=0.007
Chao1
D21
D59
High trp
D
Taxa summary (phylum)
Low trp
Relative abundance
Proteobacteria
Bacteroidetes
Firmicutes
Verrucomicrobia
Other
D21
D59
E
Taxa summary (phylum)
High trp
Relative abundance
Proteobacteria
Bacteroidetes
Firmicutes
Verrucomicrobia
Other
D21
D59
F
Significant taxonomy (species)
Low trp
Firmicutes
Bacteroidetes
Cyanobacteria
Proteobacteria
Actinobacteria
Row z-score
Allobaculum sp.
Unc. Clostridiaceae
Adlercreutzia sp.
Unc. Christensenellaceae
Dehalobacterium sp.
Alkalibacterium sp.
Streptococcus luteciae
Bifidobacterium pseudolongum
Desulfovibrio C21_c20
Unc. Rikenellaceae
Bacteroides acidifaciens
Bacteroides sp.
Bacteroides uniformis
Unc. RF32
Acinetobacter johnsonii
Erwinia dispersa
Sutterella sp.
Unc. YS2
Blautia producta
SMB53 sp.
Unc. Lachnospiraceae
Unc. Coriobacteriaceae
Fusibacter sp.
Gemella sp.
Streptococcus sp.
Enterococcus sp.
Turicibacter sp.
Staphylococcus sp.
Parabacteroides sp.
D21
D59
G
Significant taxonomy (species)
High trp
Firmicutes
Bacteroidetes
Proteobacteria
Actinobacteria
Row z-score
Allobaculum sp.
Adlercreutzia sp.
Unc. Christensenellaceae
Unc. [Mogibacteriaceae]
Dehalobacterium sp.
rc4-4 sp.
Unc. Peptococcaceae
Aerococcus sp.
Facklamia sp.
Jeotgalicoccus psychrophilus
Corynebacterium stationis
Sutterella sp.
Blautia sp.
Blautia producta
[Ruminococcus] gnavus
Dorea sp.
Anaerotruncus sp.
Enterococcus sp.
Lactobacillus sp.
Staphylococcus sp.
D21
D59

Figure S2. Gluten treatment shifts gut microbiota of NOD/DQ8 mice regardless of diet intervention. A. Principal coordinate analysis based on bacterial *16S rRNA* gene sequence abundance in fecal content of NOD/DQ8 mice fed with low or enriched tryptophan (Trp) diet before (D21), and after gluten treatment (D59), based on UniFrac distance matrices. **B**. Alpha-diversity of fecal microbiota of NOD/DQ8 mice fed with low tryptophan diet before (D21; n=10) and after gluten treatment (D59; n=10). **C**. Alpha-diversity of fecal microbiota of NOD/DQ8 mice fed enriched tryptophan diet before (D21; n=9) and after gluten treatment (D59; n=8). **D**. Relative abundance, at the phylum level, in NOD/DQ8 mice fed a low tryptophan diet before (D21; n=10), and after gluten treatment (D59; n=10). **E**. Relative abundance, at the phylum level, in NOD/DQ8 mice fed enriched tryptophan diet before (D21; n=9), and after gluten treatment (D59; n=8). **F**. Heat map of the significant species in feces of NOD/DQ8 mice fed a low tryptophan diet before (D21) and after gluten treatment (D59). **G**. Heat map of the significant species in feces of NOD/DQ8 mice fed enriched tryptophan diet before (D21), and after gluten treatment (D59). Each dot represents an individual mouse and data presented as median with interquartile range and whiskers extending from minimum to maximum. Differences in microbial composition calculated by PERMANOVA using unweighted UniFrac distance, and significant differences between taxa evaluated by two-tailed Student's two-tailed *t*-test or Wilcoxon test and multiple testing was corrected via false discovery rate (FDR) estimation.

Figure S3

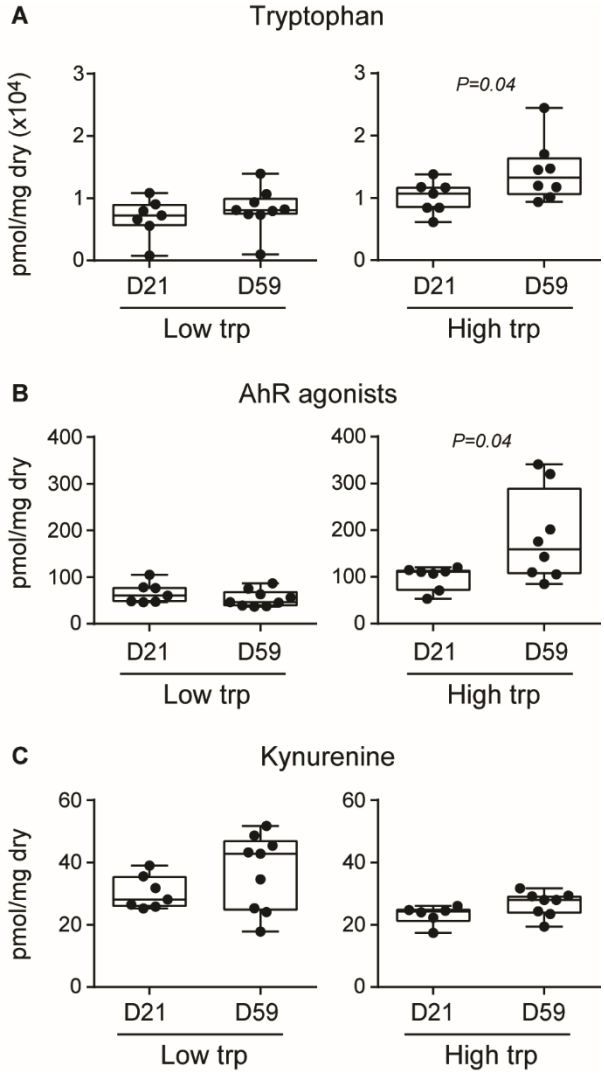

Figure S3. Fecal tryptophan and AhR agonist levels before and after gluten treatment in NOD/DQ8 mice. A-C. Quantification of **(A)** tryptophan, **(B)** total AhR agonists (tryptamine, indole-3-aldehyde and indole-3-lactic acid) and **(C)** kynurenine in feces of NOD/DQ8 mice fed with low (n=7-9) or enriched tryptophan diet (n=6-8) before or after gluten treatment (gluten sensitization and challenge). Each dot represents an individual mouse and data presented as median with interquartile range and whiskers extending from minimum to maximum. Statistical significance determined by Student's two-tailed *t*-test, or Mann-Whitney.

Figure S4

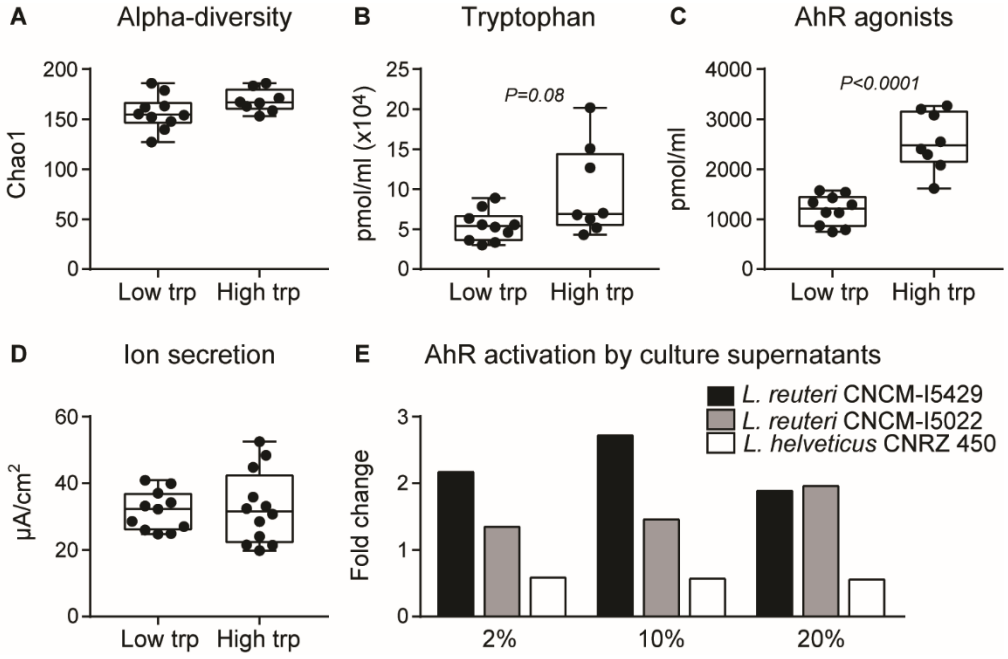

Figure S4. Tryptophan supplementation increases AhR agonists in serum of gluten treated NOD/DQ8 mice. A. Alpha-diversity of fecal microbiota of gluten treated NOD/DQ8 mice fed a low (n=10) or enriched tryptophan (Trp) diet (n=8). **B-C.** Serum quantification of (**B**) tryptophan and **(C)** total AhR agonists (tryptamine, indole-3-aldehyde and indole-3-lactic acid) in gluten treated NOD/DQ8 mice fed a low (n=10) or enriched tryptophan diet (n=8). **D**. Small intestinal barrier function assessed by ion secretion (µA/cm^2) in gluten treated NOD/DQ8 mice fed a low (n=11) or enriched tryptophan diet (n=12). **E**. AhR activation by culture supernatants (2%, 10% and 20%) from *L. reuteri* CNCM-I5429 and *L. reuteri* CNCM-I5022 relative to that by supernatants from *L. helveticus* CNRZ 450, a lactobacillus strain which does not produce AhR ligands. Each dot represents an individual mouse and data presented as median with interquartile range and whiskers extending from minimum to maximum. Statistical significance determined by Student's two-tailed *t*-test, Wilcoxon, or Mann-Whitney.

Figure S5

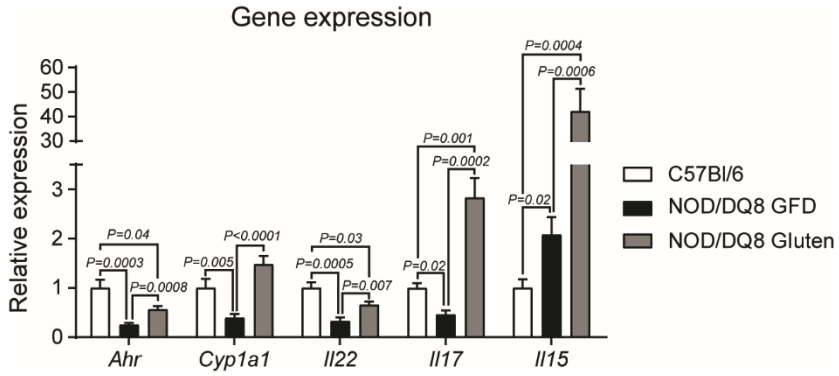

Figure S5. AhR and AhR pathway genes expression in C57Bl/6 and NOD/DQ8 mice. *Ahr*, *Cyp1a1*, *Il22*, *Il17* and *Il15* gene expression in proximal small intestine of C57Bl/6 mice fed a normal chow (containing gluten) and NOD/DQ8 mice. NOD/DQ8 mice were maintained on a gluten free diet (NOD/DQ8 GFD) or were sensitized and challenged with gluten (NOD/DQ8 Gluten) as described in the Materials and Methods (n=5-8 per genotype). Data presented as mean + SEM and statistical significance determined by Student's two-tailed *t*-test.

Figure S6

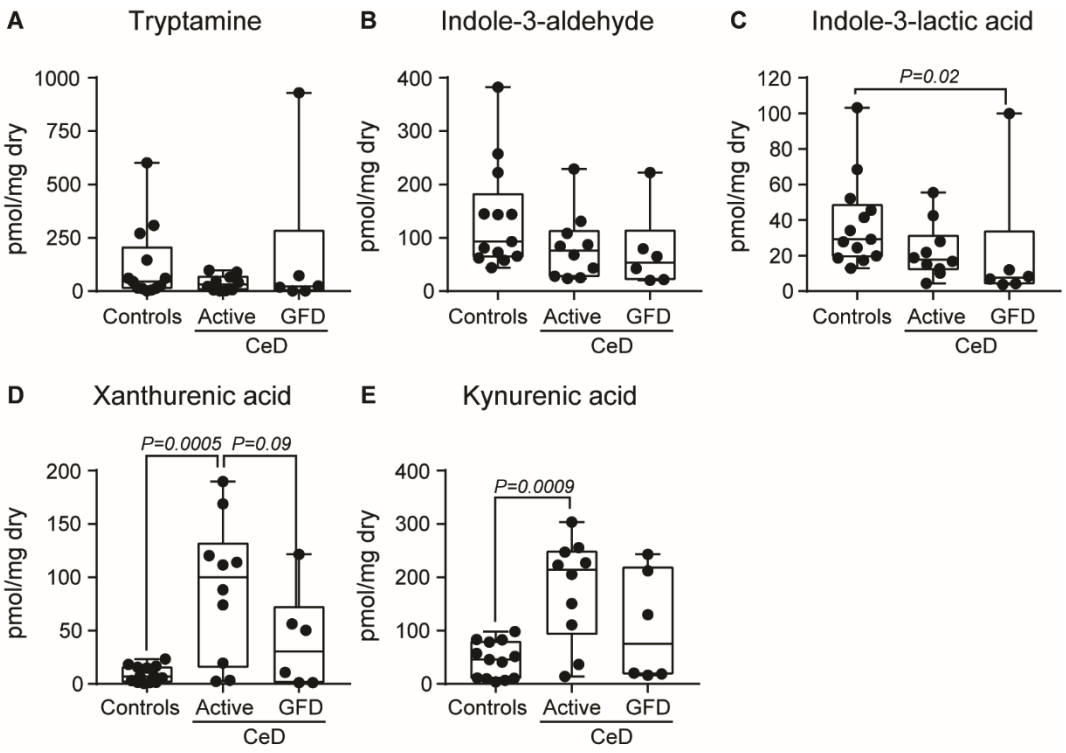

Figure S6. Patients with active celiac disease have lower fecal levels of AhR agonists and higher kynurenine metabolites. A-E. Quantification of (**A**) tryptamine (**B)** indole-3-aldehyde, (**C)** indole-3-lactic acid, (**D**) xanthurenic acid and (**E**) kynurenic acid in fecal samples of patients with active (n=10) or treated (n=6) celiac disease (CeD) and non-celiac controls (n=13). Each dot represents an individual human subject and data presented as median with interquartile range and whiskers extending from minimum to maximum. Statistical significance determined by one-way ANOVA with Tukey *post hoc* test or Kruskal–Wallis followed by a Dunn's *post hoc* test or Mann-Whitney.

Figure S7

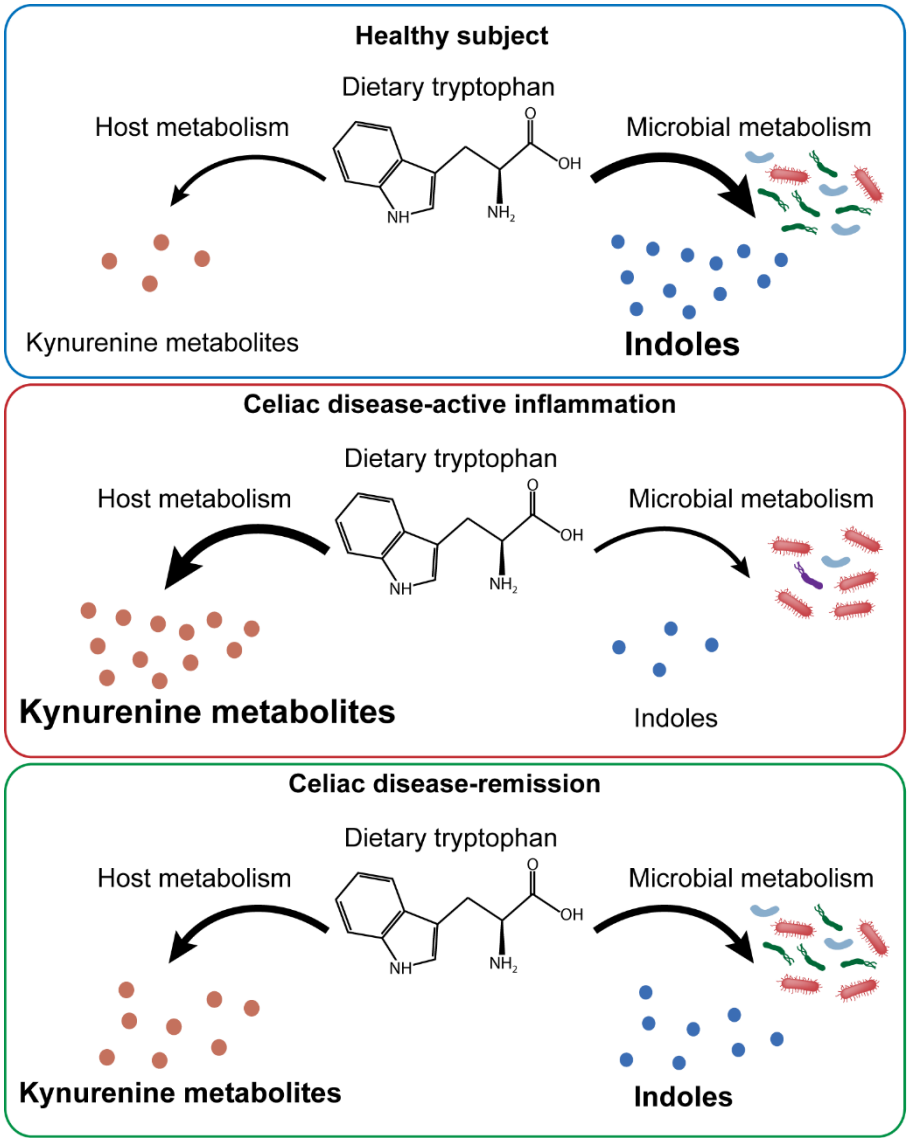

Figure S7. Proposed model for the gut Trp metabolism in CeD patients. In healthy subjects, the Trp provided by food is mainly metabolized by the gut microbiota into indoles able to activate AhR. Conversely, in patients with active CeD, the intestinal Trp metabolism shifts toward the kynurenine pathway implicated in chronic inflammatory diseases. The impaired Trp metabolism is partially restored in CeD patients in histological remission and 2-years on a gluten-free diet, resulting in reduced inflammation-inducing kynurenine production and increased microbiota-dependent AhR agonist production.

Table S1. Low and High tryptophan (Trp) diet composition

Teklad diet number **Diet short name**	**TD.170282** **Low Trp**	**TD.170282** **High Trp**
	g/kg	g/kg
Sucrose	344.5	348.68
Corn starch	150	150
Maltodextrin	150	150
Soybean oil	80	80
Cellulose	30	30
Mineral mix, AIN-93M-MX (94049)	35	35
Calcium phosphate, monobasic, monohydrate	8.2	8.2
Vitamin mix, AIN-93M-VX (94047)	19.5	19.5
Choline Bitartrate	2.7	2.7
TBHQ, antioxidant	0.02	0.02
Red food color	0.1	-
Yellow food color	-	0.1
L-Alanine	3.5	3.5
L-Arginine HCl	12.1	12.1
L-Asparagine	6	6
L-Aspartic Acid	3.5	3.5
L-Cysteine	3.5	3.5
L-Glutamic acid	41.18	28
Glycine	23.3	23.3
L-Histidine HCl, monohydrate	4.5	4.5
L-Isoleucine	8.2	8.2
L-Leucine	11.1	11.1
L-Lysine HCl	18	18
L-Methionine	8.2	8.2
L-Phenylalanine	7.5	7.5
L-Proline	3.5	3.5
L-Serine	3.5	3.5
L-Threonine	8.2	8.2
L-Tryptophan	1	10
L-Tyrosine	5	5
L-Valine	8.2	8.2
Protein (% by weight)	15.4	15.3
Protein (% kcal from)	15.6	15.6
Carbohydrate (% by weight)	64.8	65.3
Carbohydrate (% kcal from)	66	66.2
Fat (% by weight)	8	8
Fat (% kcal from)	18.3	18.3
Kcal/g	3.9	3.9

*Diets are an isonitrogenous/isocaloric modification of TD.01084.

Table S2. qPCR primers used for gene expression analysis.

Human		
Gapdh	FW	5'-CGGAGTCAACGGATTTGGTCGTAT-3'
	RV	5'-AGCCTTCTCCATGGTGGTGAAGAC-3'
Ahr	FW	5'-CCACTTCAGCCACCATCCAT-3'
	RV	5'-AAGCAGGCGTGCATTAGACT-3'
Il17a	FW	5'-AACCGATCCACCTCACCTTG-3'
	RV	5'-TCTCTTGCTGGATGGGGACA-3'
Il22	FW	5'-CGTTCGTCTCATTGGGGAGA-3'
	RV	5'-ACATGTGCTTAGCCTGTTGC-3'
Il15	FW	5'-GGCCCAAAGCACCTAACCTAT-3'
	RV	5'-TGCATCTCCGGACTCAAGTG-3'
Cyp1a1	FW	5'-CTACCCAACCCTTCCCTGAAT-3'
	RV	5'-CGCCCCTTGGGGATGTAAAA-3'
Ahrr	FW	5'-GGCTGCTGTTGGAGTCTCTT-3'
	RV	5'-CATCGTCATGAGTGGCTCGG-3'
Mouse		
Gapdh	FW	5'-AACTTTGGCATTGTGGAAGG-3'
	RV	5'-ACACATTGGGGGTAGGAACA-3'
Ahr	FW	5'-GAGCTTCTTTGATGGCGCTG-3'
	RV	5'-GTCCACTCCTTGTGCAGAGT-3'
Il17a	FW	5'-TTTAACTCCCTTGGCGCAAAA-3'
	RV	5'-CTTTCCCTCCGCATTGACAC-3'
Il22	FW	5'-CATGCAGGAGGTGGTACCTT-3'
	RV	5'-CAGACGCAAGCATTTCTCAG-3'
Il15	FW	5'-CATTTTGGGCTGTGTCAGTG-3'
	RV	5'-GCAATTCCAGGAGAAAGCAG-3'
Cyp1a1	FW	5'-ACATTGTGCCTGCCTCCTAC-3'
	RV	5'-GTAGGGTGAACAGAGGTGCC-3'
Ahrr	FW	5'-CCATTCAGAAGCGCCTTGCAG-3'
	RV	5'-AGGCAGCGAACACGACAAAT-3'
Il6	FW	5'-TGTGCAATGGCAATTCTGAT-3'
	RV	5'-CCAGAGGAAATTTTCAATAGGC-3'

FW = Forward sequence.

RV= Reverse sequence.

Table S3. Characteristics of the subjects and clinical cohort.

Diagnosis	HLA	Age	Sex	Anti-TG2 IgA*	Marsh scale	Bristol Scale
CeD-active	Not determined	33	M	Positive	3c	6
CeD-active	Not determined	26	F	Positive	3a	5
CeD-active	DQ2 homozygous	46	M	Positive	3a	5
CeD-active	Not determined	34	F	Positive	3a	6
CeD-active	DR3-DQ2 heterozygous	55	M	Positive	3c	4
CeD-active	DR3-DQ2 heterozygous/ DR4-DQ8 heterozygous	37	F	Positive	3a	7
CeD-active	DR3-DQ2	30	F	Positive	3a	4
CeD-active	DQ2 homozygous	31	F	Positive	3b	5
CeD-active	DR3-DQ2	52	M	Positive	3a	5
CeD-active	DQ2 homozygous	29	F	Positive	3a	6,7
CeD-active	DQ2 homozygous	32	F	Positive	3a	2,3,4
CeD-GFD	DR3/DR7-DQ2 homozygous	23	F	Negative	Normal	2
CeD-GFD	DR3-DQ2 heterozygous	27	F	Negative	Normal	6,7
CeD-GFD	DR3-DQ2 heterozygous	52	M	Negative	Normal	6
CeD-GFD	DR3-DQ2 homozygous	54	M	Negative	Normal	5
CeD-GFD	DR3-DQ2 heterozygous	29	F	Negative	Normal	3,6
CeD-GFD	DR7-DQ2/DQ7 heterozygous	27	F	Negative	1	5
Control	Not determined	45	F	Negative	Normal	6
Control	Not determined	50	M	Negative	Normal	4
Control	Not determined	53	M	Negative	Normal	2
Control	Not determined	39	F	Negative	Normal	6
Control	Not determined	42	M	Negative	Normal	6
Control	DR3-DQ2 heterozygous	72	F	Negative	Normal	4
Control	DR4-DQ8 heterozygous	72	F	Negative	Normal	6
Control	Not determined	63	F	Negative	Normal	4
Control	Negative	60	M	Negative	Normal	2
Control	Not determined	51	F	Negative	Normal	6
Control	Not determined	63	F	Negative	Normal	2
Control	Not determined	63	M	Negative	Normal	2
Control	Not determined	45	M	Negative	Normal	1
Control	Not determined	18	F	Negative	Normal	4
Control	Negative	45	F	Negative	Normal	6
Control	DR7-DQ2 heterozygous	36	M	Negative	Normal	6
Control	Not determined	63	M	Negative	Normal	3
Control	DR11-DQ7 heterozygous	51	F	Negative	Normal	6

CeD, celiac disease; GFD, gluten-free diet; TG2, tissue transglutaminase

*Result of >4 using TG2 ELISA from Immco Diagnostics was considered positive.